Summer 2012

Control and operation of multiple distributed generators in a microgrid

Shyam Naren Bhaskara

Department:

CONTROL AND OPERATION OF MULTIPLE DISTRIBUTED GENERATORS IN A MICROGRID

by

SHYAM NAREN BHASKARA

A THESIS

Presented to the Faculty of the Graduate School of the

MISSOURI UNIVERSITY OF SCIENCE AND TECHNOLOGY

In Partial Fulfillment of the Requirements for the Degree

MASTER OF SCIENCE IN ELECTRICAL ENGINEERING

2012

Approved by

Dr. Badrul H. Chowdhury, Advisor
Dr. Mariesa L. Crow
Dr. Jonathan Kimball

ABSTRACT

Small sized synchronous generator based distributed generators (DG) often have low start-up times, and can serve as dispatchable generators in a microgrid environment. The advantage is that it allows the power network to operate in a true smart grid environment. The disadvantage is that such DGs typically tend to have low inertia and the prime movers driving these resources need to be controlled in real time for them to operate effectively in islanded, grid-connected modes and during transition from grid-connected mode to islanded mode and vice versa. When multiple DGs are present in the microgrid, the overall control can become complicated because of the need for sharing the resources. A smart grid environment is then necessary to control all dispersed generation sources in the microgrid. The most common control strategy adopted for multiple DGs connected to a network is droop control. Droop control ensures that the load needed to be served is shared by all the generators in the network in proportion to their generating capability. When DGs operate in a microgrid environment, there is a need for coordinated operation between the DGs, the utility grid and the loads. A MicroGrid Central Controller (MGCC) can keep track of the status from the system standpoint and command the local Microsource Controllers (MC) to ensure system stability. In various modes of operation like grid connected, islanding and during transition, the MGCC can support the MCs by giving them necessary information to contribute towards stable operation.

ACKNOWLEDGMENTS

I sincerely extend my deepest sense of gratitude to my mentor and advisor Prof. Badrul Chowdhury for his support and invaluable guidance. This thesis would not have been possible without his patience and constant motivation. I am also grateful to Ameren Corporation for providing me with a research assistantship to prepare state-of-the-art technologies report on Microgrids which helped me set objectives for my thesis and achieve them.

I would also like to thank Prof. Mariesa L. Crow and Dr. Jonathan Kimball for serving on my graduate committee. I would also like to profoundly thank Prof. Keith Corzine for guiding me through the process of setting up the laboratory microgrid. A special thanks to Md. Rasheduzzaman for working with me during the course of this thesis.

Finally, I would like to dedicate this thesis to my loving parents Dr. B. Sivarama Sarma and Mrs. Lakshmi Krishna Latha and my brother Siddhartha for giving me all the support and encouragement to pursue a Masters in Electrical Engineering.

TABLE OF CONTENTS

Page

APPENDICES

LIST OF ILLUSTRATIONS

Page

LIST OF TABLES

Page

NOMENCLATURE

Symbol	*Description*
DER	Distributed Energy Resource
DG	Distributed Generator
MC	Microsource Controller
MGCC	Microgrid Central Controller
PCC	Point of Common Coupling
LC	Load Controller
FPC	Federal Power Commission
PUHCA	Public Utility Holding Company Act
MIC	Measurement, Information and Control
EPS	Electric Power System
IM	Induction Machine

1. INTRODUCTION

1.1. MOTIVATION

With the increasing demand of power, the burden on the transmission network is increasing at an unexpected pace. Updates to the transmission network are economically challenging. Furthermore, the depletion of fossil fuels and the rampant increase in the price of these fossil fuels have resulted in increased interest to include renewable sources of energy for power production. Recent natural calamities have made several nations to reconsider investing and depending on nuclear power. As a result, there is a great need for including wind, solar, fuel cells and other types of energy sources as major contributors to the power system. The most challenging aspect of including such sources is their intermittency. There is also need for introducing energy storage devices such as battery and flywheels to enhance the stability of the system.

Microgrids have emerged as a suitable solution to tackle all these issues. They enable distributed generation and hence are capable of deferring network upgrades. They can facilitate grouping of the various kinds of sources into smaller subsets which are easier to manage and operate. Apart from these advantages, microgrids also enable islanded operation when there is a fault in the sub-transmission network. The biggest concern with microgrids is its stability. It does not have the luxury of a large power system which can absorb the transients and recover from faults. This thesis investigates inclusion of synchronous machine based DGs to enhance transient stability and smooth transition between islanded and grid connected modes of operation.

1.2. OUTLINE

A discussion on the background of distributed generators, microgrids, and synchronous machines is presented in Section 2.

Section 3 describes the synchronous machine microsource controller. The control strategies during different modes of operation are discussed in detail.

Section 4 comprises of details of the laboratory microgrid test system. Details of the various hardware equipment used for building the microgrid are provided. Further, the microsource controller and microgrid central controller development is elaborated and the algorithms are discussed.

Section 5 presents the test results for various tests performed on the microgrid. Operating procedures for the microgrid are defined and various factors affecting microgrid performance are studied.

Future work and conclusions are described in Section 6.

2. BACKGROUND

2.1. DISTRIBUTED GENERATION

With the increasing demand of power, the need for commissioning new generating units is increasingly becoming a necessity. Apart from the heavy investment and the complexities involved in setting up large generating stations, setting up of new generating units call for upgrades to the transmission network to transport the power generated to the load centers. Updates to the transmission network are economically constraining, and therefore, distributed resources are being considered to avoid these problems [1].

Distributed energy resources (DER) are defined as demand- and supply-side resources that can be deployed throughout the electric distribution system to meet the energy and reliability needs of the customers served by that system. Distributed generators (DG) refer to small sources of electric power generation or storage (typically ranging from less than a kW to tens of MW) that is not a part of a large central power system and is located close to the load. DG has several advantages when connected to the electric power system including combined heat and power plants yielding high efficiency, standby/emergency generation resulting in enhanced efficiency, peak shaving, grid investment deferment and premium power. At the same time islanding, voltage regulation, harmonics, modified power flows, protection and metering are some of the major issues concerning DGs [2]. A better way to realize the emerging potential of distributed generation is to take a system approach which views generation and associated loads as a subsystem or a “microgrid” [3].

2.2. MICROGRID

2.2.1. Definition. Microgrids are power systems that can operate autonomously using combinations of conventional generation technologies such as diesel gensets and combined heat and power systems, renewable resources, other new generation technologies, such as micro-turbines and fuel cells, energy storage systems, and load management systems. In many ways, a microgrid is really just a small-scale version of the traditional power grid that the vast majority of electricity consumers in the developed world rely on for power service today. IEEE Std. 1547.4-2011 [4] defines DER island systems or microgrids as electric power systems (EPS) that: have DER and load, have the ability to disconnect from and parallel with the area EPS, include the local EPS and may include portions of the area EPS and are intentionally planned.

Figure 2.1 shows a low voltage (LV) microgrid that connects to the medium voltage (MV) network through a transformer through the microgrid central controller

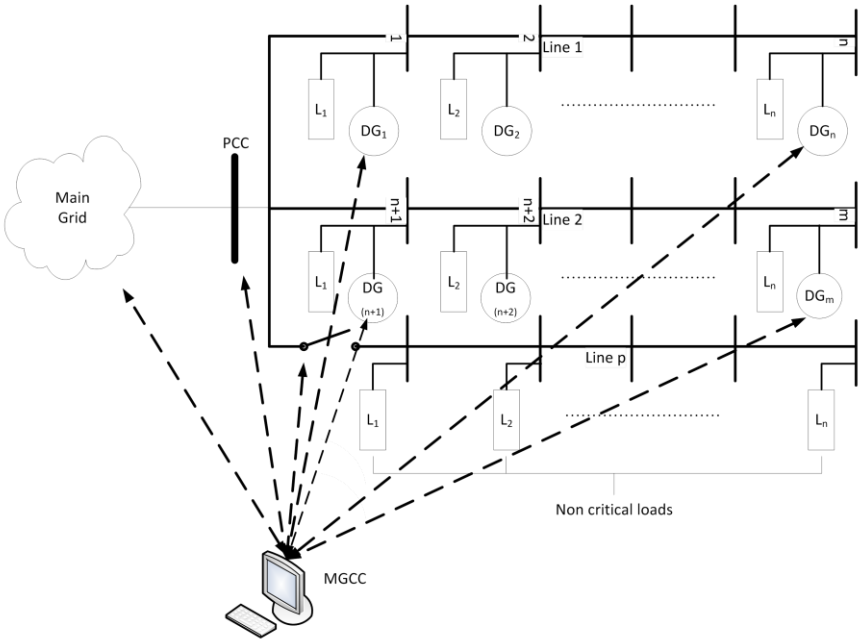

Figure 2.1 Typical Microgrid System

(MGCC) at the point of common coupling (PCC). The microgrid comprises of various DGs such as CHP, PV and microturbines, and energy storage resources such as batteries and fuel cells. Every distributed generator is connected to the microgrid through a microsource controller (MC) and the load is connected through a load controller (LC) [5].

There are several benefits to microgrids [6]. Microgrid is described as a tool for sustainable energy [7]. Firstly, microgrids facilitate connection of distributed generation (DG) and high penetration of renewable energy sources. They also facilitate cogeneration in a combined heat and power (CHP) system [8]. They increase power quality and reliability of electric supply. They defer network investments. They contribute to adequacy of generation because of its ability to control internal loads and generation. They also support the electrical network in remote sites and rural areas [9].

There are also economic benefits from microgrids [10]. Barker, et al [11] have estimated the cost of power from microgrids with DG support to be 10 ¢/kWh as opposed to 10.5¢/kWh in the case of conventional power.

The necessity of microgrids can be understood from the article in PEI magazine [12] which quotes that the vision of DOE for smart grids to improve power quality with more control and awareness of the operational state of the electric system at affordable prices cannot be achieved either until the T&D system is fixed or microgrids come into existence. Venkatramanan et al [13] present a growth model wherein the various features and barriers for microgrids have been identified.

The other reasons for such recognition for microgrid over recent times have been because of increased awareness for the environmental concerns and the ever increasing price for fossil fuels which has resulted in the increased attention towards implementing

renewables into power systems. Also there is a high priority for countries to have energy security. All these reasons have increased governments' interest in microgrids.

At the same time, several obstacles have also been identified for the growth of microgrids which need to be addressed [4]. Lack of established regulatory policies and a solid regulatory base in place in the United States is a major hurdle. Pudjianto et al [14] present a review of the regulatory situation in Netherlands, United Kingdom and Spain. At the same time there are certain legal issues, such as the Public Utility Holding Company Act (PUHCA) in the United States which mandates that sale of electricity for resale in interstate commerce would turn the seller into a public utility and require filings with the Securities and Exchange Commission (SEC) and the Federal Power Commission (FPC). Also, King [15] presents results of a survey involving the staff representing 26 different state PUCs and the PUC of the district of Columbia concerning the legality of microgrids, interaction between microgrids and utilities and regulatory oversight of microgrids and microgrid firms.

2.2.2. Modes of Operation. Four modes of operation have been identified by IEEE Std. 1547.4-2011 [4], namely: area grid connected mode, transition-to-island mode, island mode, and reconnection mode.

In the grid connected mode, it is advised that the Measuring, Information exchange and Control (MIC) equipment needs to be in operation to make system related information available including protection device status, generation levels, local loads, and system voltages, to the island control scheme such that a transition can be planned in advance.

During the transition-to-island mode, it is advised that enough DER and DER of the correct type (DER conforming to all the IEEE Std. 1547.4 [4]) is ensured to be

available to support the system voltage and frequency for whatever time the island interconnection device and protective relaying take to effect a successful transition. Also, if sufficient DER and DER of the correct type are not present, then black start capability needs to be provided inside the island. Pedrasa, et al [16] identifies some more issues such as balance between supply and demand, power quality, communication among microgrid components and micro-source issues like lack of inertia, lack of spinning reserves and slow response or ramp time.

During the island mode, it is suggested that one or more participating DER will need to be operated outside the IEEE 1547 voltage regulation requirement to assure DER island system voltage and frequency stability. Also, there should be adequate reserve margin that is a function of the load factor, the magnitude of the load, the load shape, the reliability requirements of the load, and the availability of DER. It is suggested that to balance the load and the generation within the island various techniques such as load-following, load management, and load shedding be used. Also, it is pointed out that transient stability should be maintained for load steps, DER unit outage, and island faults. It is also suggested that adaptive relaying may be implemented to provide adequate protection for a variety of system operating modes. Bollen, et al [17] propose standard operating ranges for frequency and voltage based on the European standard EN50160 for interconnected and islanded systems. It is proposed that for interconnected systems, the frequency shall be between ±5 Hz during 99.5% of the year and always between -3 and +2 Hz of the nominal frequency. For islanded systems, the frequency shall be always between ±1 Hz during 95% of one week and always between ±7.5 Hz. The voltage for island operation lasting less than 10 minutes shall be between 85% and 110% of the declared voltage.

For reconnection of the DER island system to the EPS, monitoring should indicate that the proper conditions exist for synchronizing the island with the EPS. It is advised that after an area EPS disturbance, no reconnection shall take place until the area EPS voltage is within Range B of ANSI/NEMA C84.1-2006, Table 1, the frequency range is between 59.3 Hz to 60.5 Hz, and the phase rotation is correct. Also, the voltage, frequency, and phase angle between the two systems should be within acceptable limits as specified in IEEE Std 1547-2003 in order to initiate a reconnection. Several ways to reconnect the DER island system back to the EPS are also mentioned.

2.3. SYNCHRONOUS MACHINE BASED MICROSOURCES

2.3.1. Necessity of Synchronous Machine Based Microsources. Synchronous machine have been used as generators for several decades in the power system. Most of the generations today are from three phase synchronous generators. Several advantages of synchronous machines have ensured the dominance of synchronous generators.

Being inertia based, synchronous machines can maintain synchronism from transient oscillations in the system. With appropriate controls in place, synchronous machines can also ensure that there is a balance of demand and supply in the system. They also have the inherent nature of operating at constant frequency. Being excited by an external DC excitation source, synchronous machines can be operated at both leading and lagging power factor. Hence, they can be used to also generate reactive power required by the system or they can be used to absorb excess reactive power and hence improve the voltage profile in the system.

Synchronous machine-based DG are normally used for combined heat and power applications [18]. Combined heat and power systems have very high energy efficiency

and reduce energy costs. Thus it is very beneficial to include synchronous machine based DGs in the microgrid.

2.3.2. Control of Synchronous Machine Based Microsources. The control system of the synchronous machines needs to ensure that the synchronous machine generates active and reactive power within the ratings of the machine at nominal voltage and frequency as demanded by the system to which it is connected. At the same time the load in the system has to be served and the machines must each generate a share of the power demanded by the load.

Active and reactive power sharing can be explained using the active and reactive power flows between two AC sources through a line impedance, Z as shown in Figure 2.2 [19].

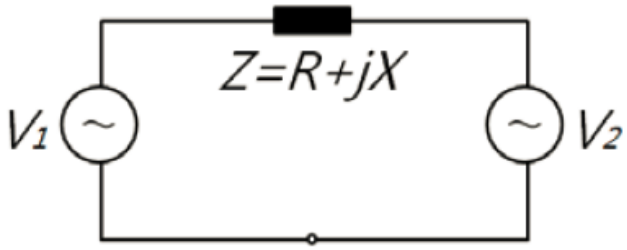

Figure 2.2. Two AC sources connected through a line

The active and reactive power flowing through the line is given by

$$P = \frac{V_1}{R^2 + X^2}[(R(V_1 - V_2\cos(\delta)) + XV_2\sin(\delta))] \quad (1)$$

$$Q = \frac{V_1}{R^2 + X^2}\left[\left(-RV_2\sin(\delta) + X(V_1 - V_2\cos(\delta))\right)\right] \quad (2)$$

For a predominantly inductive line, the phase angle between the two voltages is very small. Hence for small δ,

$$P = \frac{V_1 V_2}{X} \sin(\delta) \tag{3}$$

$$Q = \frac{V_1}{X}(V_1 - V_2) \tag{4}$$

Thus, the active power is proportional to the phase angle and the reactive power is proportional to the voltage difference between the two systems. Hence, a DG can control its active power by controlling the frequency at which it is generating and the reactive power by controlling the voltage at its terminal.

From the synchronous machines view point, two inputs that can be used as control parameters are torque applied by the prime mover to the shaft of the machine and the voltage across the field winding of the synchronous machine. The torque applied controls the speed of the shaft affecting the frequency of the power generated by the machine, and hence, the active power generated by the machine. The field voltage controls the terminal voltage, and hence, the reactive power generated by the machine.

3. SYNCHRONOUS MACHINE CONTROLLER DESIGN

In a microgrid environment, the synchronous machine will be required to operate in different scenarios or modes. In the grid connected mode, the machine is connected to an infinite bus such as the EPS, and the voltage and frequency are no longer the control objectives of the machine control system, and remain fixed irrespective of the torque and the field voltage applied. Thus, we need to use the shaft torque and the field voltage as tools to modulate the output active and reactive powers of the machine. In the islanded mode, it will be the responsibility of the control system to ensure nominal voltage and frequency apart from delivering the required amount of power to the system. Thus depending on the mode of operation of the microgrid, the control system for the synchronous machine will have to change its control strategy to fulfill the needs of the operating mode.

3.1. CONTROL STRATEGY DURING DIFFERENT MODES OF OPERATION

3.1.1. Control During Islanded Mode – Droop Control. During islanded mode, the objective is to ensure that the required amount of power is delivered at the nominal voltage and frequency. It is also important to ensure that the machines in the microgrid do not loose synchronism. Also, when multiple synchronous generators are present in the system, there should be a provision for sharing the power demanded by the load taking the machine ratings into consideration.

Typically frequency is reduced or "drooped" with increasing generated active power and voltage is drooped with increasing generated reactive power. Droop control has been extensively used with synchronous machines when multiple synchronous machines are supplying power and need to maintain nominal voltage and frequency

within the entire system. In the context of microgrids, since we need to control both the active and reactive power, two different droop controls need to be used. The first one being active power-frequency droop (P/ω droop) and the second one being, reactive power-voltage droop (Q/V droop) [20–24].

First, let us consider a single machine serving a load as shown in Figure 3.1. A prime mover PM is driving the shaft of a synchronous machine SM which is connected to a load. As described above, the shaft torque and field voltage have to be used to control the synchronous machine such that the machine serves the load at nominal voltage and frequency. According to the theory of droop control, Equations (5) and (6) can be used to

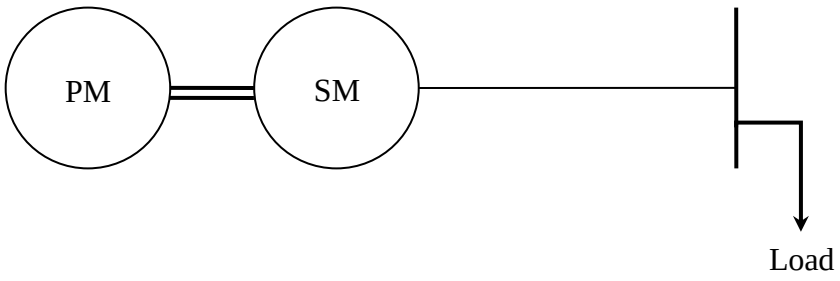

Figure 3.1. Single generator serving a load

calculate the commanded shaft speed and terminal voltage from the active (P_{gen}) and reactive (Q_{gen}) power being generated by the machine. D_{pf} and D_{QV} are the droop coefficients for the active and reactive power droop curves. ω_{rm0} and V_{s0} are the speed and the terminal voltage at no load. They also represent the base speed and terminal voltage of the machine. $P_{gen,rated}$ and $Q_{gen,rated}$ are the rated active and reactive power of the machine.

$$\omega_{rm}^{*} = \omega_{rm0}\left(1 - \frac{D_{pf}}{100} \times \frac{P_{gen}}{P_{gen,rated}}\right) \quad (5)$$

$$V_{s}^{*} = V_{s0}\left(1 - \frac{D_{QV}}{100} \times \frac{Q_{gen}}{Q_{gen,rated}}\right) \quad (6)$$

The variation of speed with the active power generated by the machine can be represented by a straight line according to Equation (5) as shown in Figure 3.2 (a). The slope of the line is the droop coefficient D_{pf}. It can be seen that at no load, the machine operates at rated speed. Once the machine starts to serve load the speed starts decreasing.

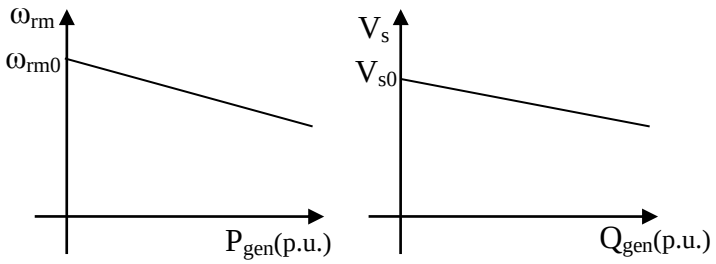

Figure 3.2. (a) P/ω droop characteristics (b) Q/V droop characteristics

Similarly, the variation of terminal voltage with the reactive power generated by the system can also be represented by a straight line according to Equation (6) as shown in Figure 3.2 (b). The slope of this characteristic is the droop coefficient D_{QV}.

Now let us consider the situation where there are multiple machines in the system. Let us consider a system where two machines are connected in parallel to a bus as shown in Figure 3.3.

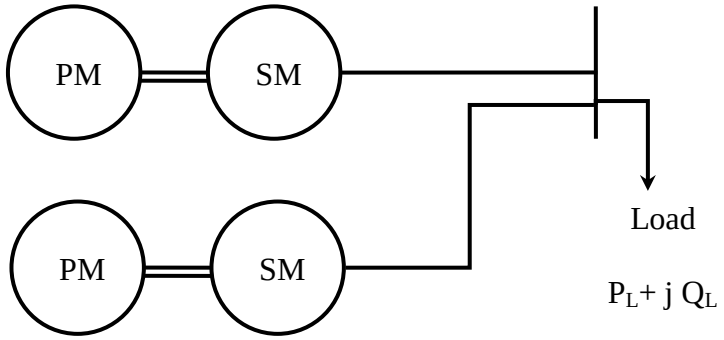

Figure 3.3. Two generators serving a load

Let us assume that generator SM_1 is rated at Pg_1 and is set to operate at a d_1% droop. Similarly, generator SM_2 is rated at Pg_2 and is set to operate at d_2% droop. Let us also assume that both the machines have a no load speed of ω_0 and the voltage at the load bus be V_L. The droop curves for the machines are shown in Figure 3.4. At steady state, let the active power generated by SM_1 be P_1 and that by SM_2 be P_2. From Equation (5), the slope of the P/ω droop characteristics of SM_1 is $\frac{d_1}{P_{g1}}$ and the slope the P/ω characteristics

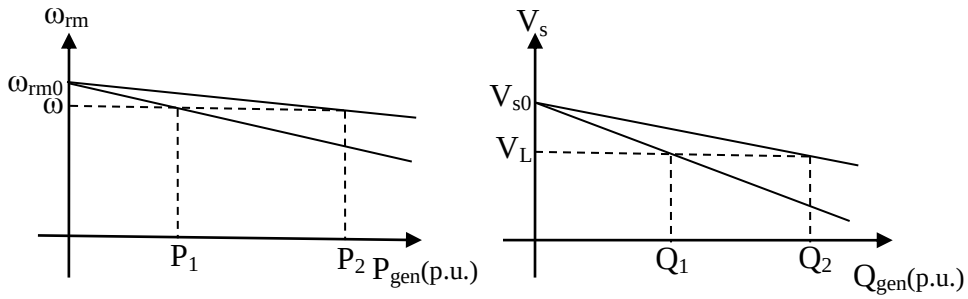

Figure 3.4. (a) P/ω droop characteristics (b) Q/V droop characteristics

of SM_2 is $\frac{d_2}{P_{g2}}$. The active power load being served by both the machines is P_L. Since the frequency at all points in an electrical system has to remain the same, the shaft speed of both the machines will have to remain the same, say ω.

Thus,

$$P_L = P_1 + P_2 \tag{7}$$

$$P_1 = \frac{\omega_{rm0} - \omega}{\left(\frac{d_1}{P_{g1}}\right)} \tag{8}$$

$$P_2 = \frac{\omega_{rm0} - \omega}{\left(\frac{d_2}{P_{g2}}\right)} \tag{9}$$

$$P_1 = \left[\frac{\left(\frac{d_2}{P_{g2}}\right)}{\left(\frac{d_1}{P_{g1}}\right)}\right] P_2 \tag{10}$$

Hence, the share of the active power load generated by each machine can be calculated as,

$$P_1 = \left(\frac{\frac{d_2}{P_{g2}} / \frac{d_1}{P_{g1}}}{1 + \frac{d_2}{P_{g2}} / \frac{d_1}{P_{g1}}}\right) P_L \tag{11}$$

Equations (9) and (7) can be used to study the effect of generator rating and droop coefficient on the share of load generated by each machine. Figure 3.5 and Figure 3.6 show the variation of share of generation by the machine with varying generator ratings and droop coefficients. The following observations can be made from the graphs.

1. The machine with higher rating generates a higher share of the power demanded.
2. The machine with lower droop coefficient generates a higher share of the power.

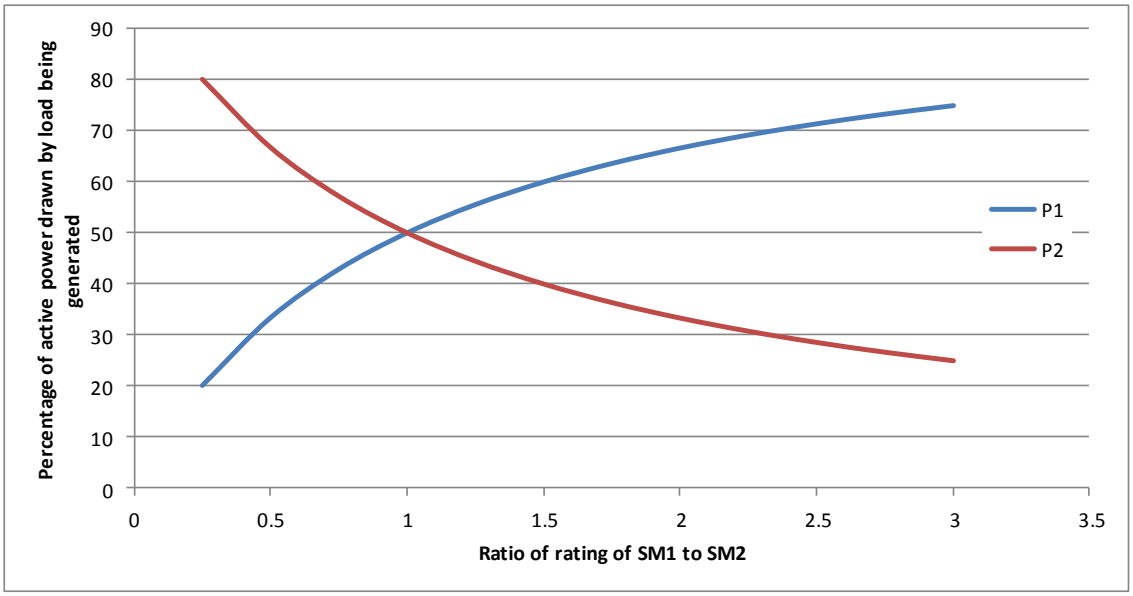

Figure 3.5. Variation of share of generation with generator ratings assuming equal droop

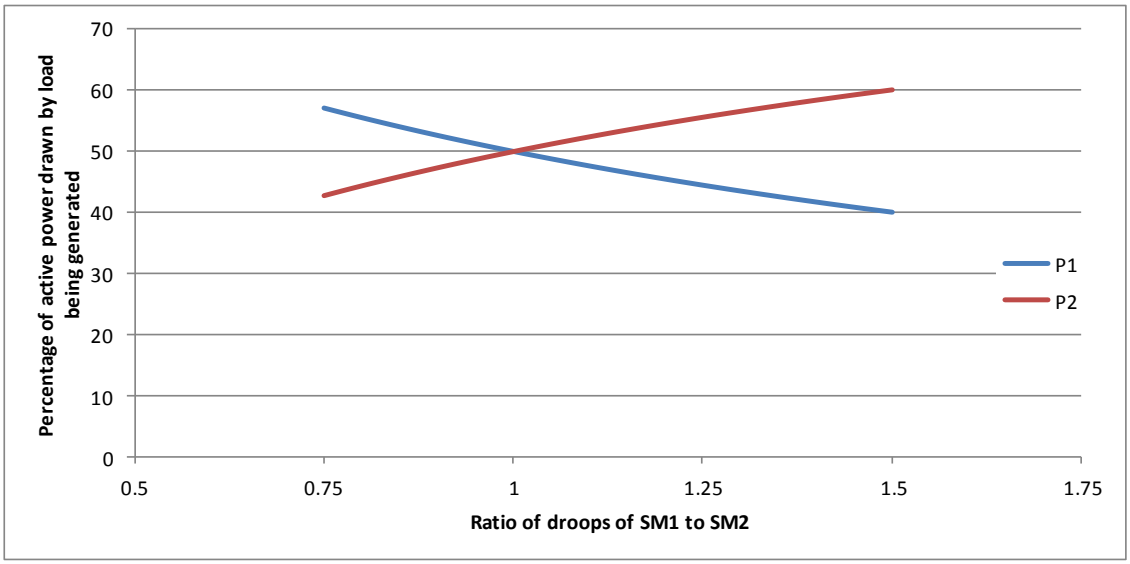

Figure 3.6. Variation of share of generation with droop assuming equal ratings

Since both generators are connected to the same bus, the share of reactive power is similar to that of the active power. But such a system might not be practically feasible

in the real world. The generators may have to be separated by some physical distance leading to a line connecting the two machines.

3.1.2. Control During Grid Connected Mode. During grid connected mode the objective of the synchronous machine controller is to control constant output power. Since the frequency is determined by the grid and is held stiff, the rotor speed is constant. As a result the power output depends directly on the torque exerted by the prime mover on the shaft. Thus the mode of operations is referred to as Constant Power Mode (CPM).

3.2. LOCAL CONTROLLER DESIGN

The local controller is responsible for maintaining stable operation of the generating units. As shown in Figure 3.7, the local controller will have to use the stator voltages, line currents and shaft speed to decide the commanded torque, τ^* and commanded field voltage, Vfd*. As explained earlier, the local controller will have to switch between constant power mode for grid connected operation and droop mode for islanded operation.

Using the stator voltages and currents, active and reactive powers delivered by the DG is calculated. In the droop mode, the commanded torque is calculated from the active power being generated by the machine, P_{gen}. Active power is passed through a droop control block. The droop control block is also fed with the no-load speed as an input. This input is used to shift the droop curves as explained earlier. The droop controller calculates the target shaft speed, ω_{rm} which is given to a PI controller which converts the target shaft speed to a commanded torque, τ^*. The DC machine is commanded to apply this torque on the shaft through the DC machine drive. Similarly the reactive power being generated is used to calculate the field voltage required to be applied to the field winding

of the synchronous machine through the programmable DC power supply. The no load voltage V_{s0}, can be used to shift the reactive power-voltage droop curve to change the voltage of the machine while in droop mode.In grid connected mode, the commanded torque is obtained from the target active power output from the generator when passed through a PI controller. Similarly the commanded field voltage is obtained from the target reactive power output from the generator.

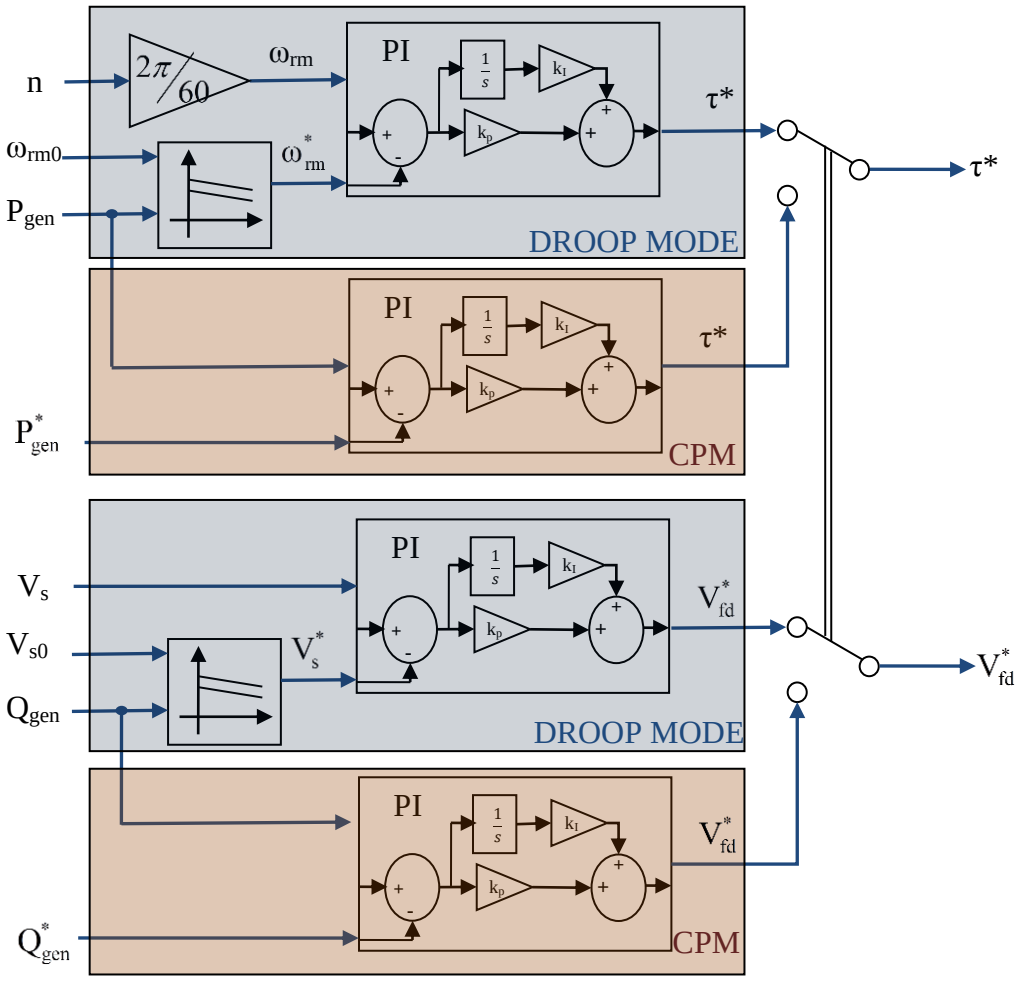

Figure 3.7 Local controller schematic

A screenshot of the LabVIEW interface for the local controller is shown in Figure 3.8. The drive conditions panel on the top-right shows the speed, armature and field currents, power drawn and the torque applied on the shaft of the DC machine drive. Below the drive conditions panel is the MGCC panel where MGCC control can be enabled/disabled. If the MGCC control is disabled, the operator can control the DG by selecting the mode of operation (Droop/CPM), and the commanded active and reactive powers. Pset and Qset display the set points received from MGCC. A list of all messages received with the date and time stamp is also recorded here. Machine armature measurements and contactor terminal measurements panels display the measured voltage, current and frequency. Active, reactive and apparent powers are calculated and displayed. The Dynamometer/System Controls panels enables the operator to operate the DG manually. For MGCC control, the control mode has to be set to Torque. The droop control panel ensures the speed of the shaft obtained from the active power-frequency droop equation. The Visualization Tabs plot speed, torque, active and reactive power, voltage, frequency and grid power flows vs. time. The field supply controls panel controls the programmable power supply. When the output is turned on and the Q~V droop is enabled, field voltage corresponding to the reactive power-voltage droop equation is commanded. The FVNR combination starter panel has controls to the contactors connected to the DG.

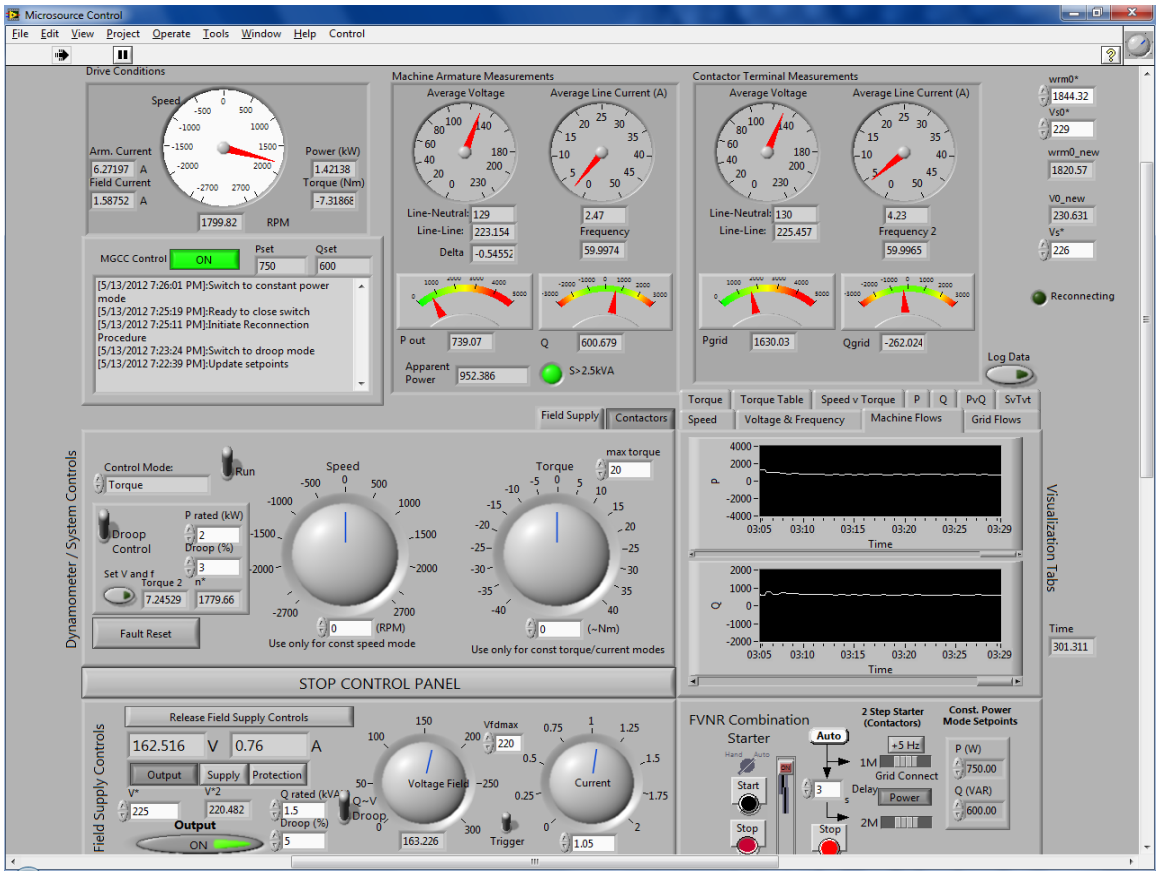

Figure 3.8 Screenshot of the microsource controller

4. MICROGRID CENTRAL CONTROLLER

4.1. RESPONSIBILITIES OF THE MGCC

Microgrids can comprise of several DGs which can be located at a distance from each other. There is a need for maintaining coordinated operation and control of all the DGs in the microgrid to maintain stability in the system and accomplish the goals of the microgrid [25]. Thus, there is a need for a supervisory controller which coordinates the operation of the local microsource controllers through a communication network. The supervisory controller or the microgrid central controller (MGCC) can receive status information from all the local controllers and monitoring systems in the microgrid and take decisions from a system point of view.

The importance of having a centralized controller like the MGCC is described in [26–29]. Some of the key facts are noted based on the literature review:

- To provide power set points for the DGs
- To ensure economic scheduling
- To supervise demand side bidding
- To control peak load during peak load hours
- To control non critical loads during islanding
- To minimize system loss
- To detect islanding conditions based on the point of common coupling (PCC) measurements
- To provide LC with the information when grid comes back for resynchronization
- To monitor power flow through local generating units and PCC

The MGCC can be very beneficial for managing the overall stability of the microgrid. Decisions such as when to island the microgrid can be crucial for the operation of the microgrid. It is important that all the microsource controllers take action on these decisions simultaneously. If such decisions are taken by the local controllers themselves then coordinated operation cannot ensured.

Figure 4.1 describes the various functionalities that the MGCC can provide for the microgrid. Since the MGCC can monitor the point of common coupling (PCC), the MGCC can analyze the power quality at the PCC and decide to island the microgrid. Islanding decisions can also be dependent on economic considerations as well. Also, the MGCC can monitor power being generated by the renewable energy sources and optimize the power generated by other sources. Further, the MGCC can keep a record of the power flows and system conditions from the past, and use those records to forecast the load and plan the generation within the microgrid ahead of time, especially when real time pricing of power is in place. For example if the MGCC can predict that there will be

Figure 4.1 Microgrid Central Controller responsibilities

an increase in demand for power after a certain time, then the batteries in the system can be charged when the cost of energy is cheap and use that energy when the demand picks up. If need be, the MGCC can decide to shed some load to ensure stable and economic operation of the microgrid [30].

The MGCC can also be used for back up protection within the microgrid. Direct connected rotating machines can be prone instability during voltage dips caused by faults in island-operated microgrid, and therefore, they may jeopardize the stability of the entire microgrid [31]. Since the MGCC is in constant communication with the entire microgrid, it can also be used as a backup protection scheme of the microgrid.

After islanding, once the grid support is restored, and it is decided to reconnect, the voltage and frequency at the PCC will have to be matched with that on the grid side. The MGCC can coordinate with multiple local controllers to instruct them to regulate their voltage and frequency to facilitate resynchronization with the grid.

4.2. MGCC ALGORITHM DEVELOPMENT

In this study, the MGCC is used to make islanding decisions and during resynchronization with the grid. Primarily, the MGCC has to be in constant communication with the various MCs and LCs in the system. It receives status data from the DGs, the switches, and other measurement units in the system. In the second process, the status data are studied and commands are generated for the microsource controllers and transmitted back to them. A flow chart for the MGCC is presented in Figure 4.2.

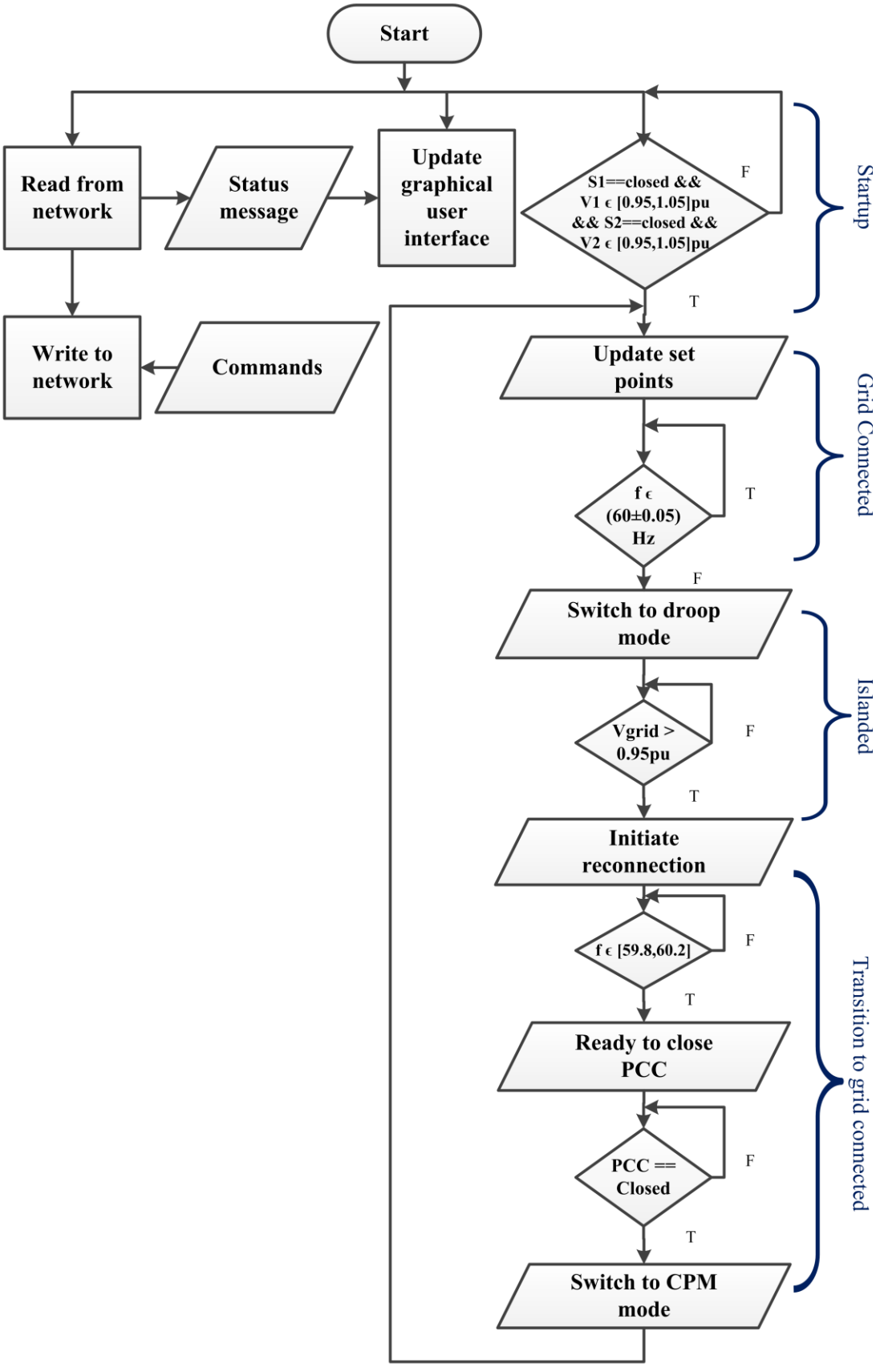

Figure 4.2. Microgrid central controller flowchart

The MGCC operating flow chart has four different objectives. These are:

1. Startup
    - Start DG units and synchronize them to their corresponding buses.
    - Track synchronization of the DGs
2. Grid connected operation
    - Monitor PCC voltage and frequency
    - Send active and reactive power set points to the local controllers
    - Monitor islanding condition
3. Islanded
    - Command local controllers to go to droop mode
    - Shed non critical load
    - Monitor PCC voltage and frequency
    - Initiate transition to grid once the grid is back
4. Transition to grid connected

These operating modes are described below:

During startup, the MGCC starts communicating with the local controllers, the PCC and non-critical load breakers. It checks if the PCC voltage is within the range of 1.05 pu to 0.95 pu as well as PCC breaker is on or off. Parallel to this event, the MGCC checks the terminal voltage of the newly started DG unit and the status of the contactor, which connects DG with the microgrid.

During grid connected mode, the MGCC commands the local controller to generate specific amounts of active and reactive power from its associated DG. At the same time, the MGCC checks if the system frequency is within ±5% of 60Hz and

monitors the grid side PCC voltage. If the system frequency is not within this band, the MGCC switches to islanded mode of operation.

During islanded mode, the MGCC sends a message to the local controllers to switch to droop mode. The MGCC continues monitoring the grid side PCC voltage and frequency. As soon as the MGCC finds that PCC side grid voltage and frequency is restored to the nominal value, it sends a message to the local controller to initiate reconnection.

Local controller receives signal from the MGCC and immediately responds to the mode by shifts the droop curve in such a way as to match the grid side frequency which is 60Hz. At the same time, the MGCC sends the information of the PCC voltage to the DGs so that, they can start to increase or decrease their terminal voltage until the microgrid side PCC voltage matches with the grid side PCC voltage. At this point The MGCC closes the PCC contactor between the microgrid and the main grid. As soon as the contactor is closed, the MGCC sends a signal to the local controllers to switch to constant power mode. The MGCC then switches to grid connected mode.

4.3. IMPLEMENTING THE MICROGRID CENTRAL CONTROLLER

The MGCC has a graphical user interface platform which shows status of the microgrid. A screenshot of the MGCC is shown in Figure 4.3. On the top of the MGCC, the current operating mode of the MGCC is defined. An interactive system diagram shows the system status information. LED indicators are provided for the grid, and the DGs to show their participation in the microgrid. Grid voltage, frequency, DG voltages and active and reactive power flows are displayed as received from their respective MCs. Contactor/switch states are also displayed on the system diagram. Load states are

calculated based on the power flows at buses 1 and 2 and are displayed on the system diagram. Above each DG, the DG status information such as torque and speed are displayed. There is also a provision for entering commanded active and reactive set points to each DG.

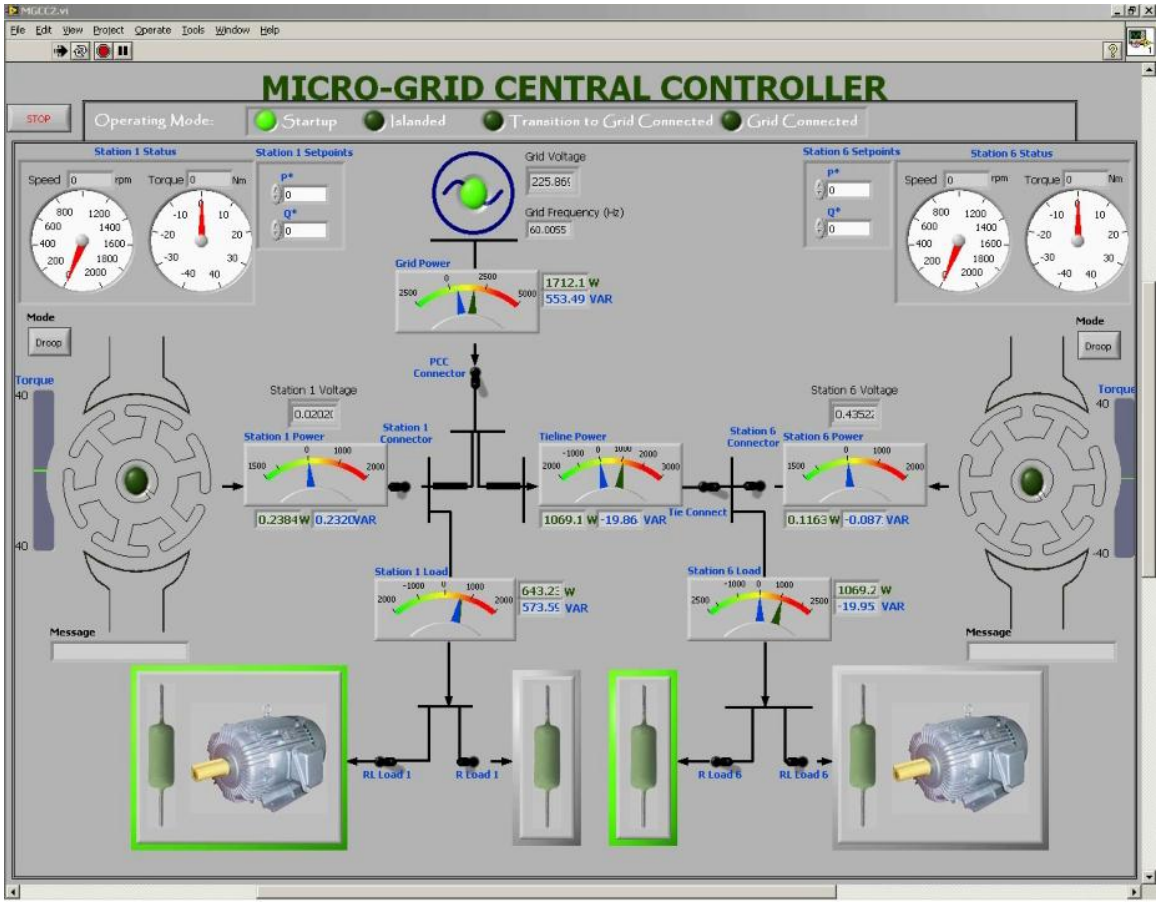

Figure 4.3 Screenshot of the Microgrid Central Controller

5. LABORATORY MICROGRID TEST SYSTEM

5.1. MICROGRID SYSTEM DESIGN

The laboratory microgrid test system comprises of two generating units (DGs). Each DG is connected to the microgrid through a contactor/switch to connect/disconnect from the microgrid. The system is a three bus system. As shown in Figure 5.1, DG1 is connected to bus 1, DG2 to bus 2 and grid to bus 3. Detailed discussion on the DGs is presented in Section 5.2. Utility grid is stepped down to 230V, the rating of the DGs and the loads and is supplied to the PCC, bus 3, through a contactor to facilitate islanding. Buses 1 and 2 are connected to bus 3 through two lines 1 and 2. Resistive and resistive inductive loads are connected to buses 1 and 2.

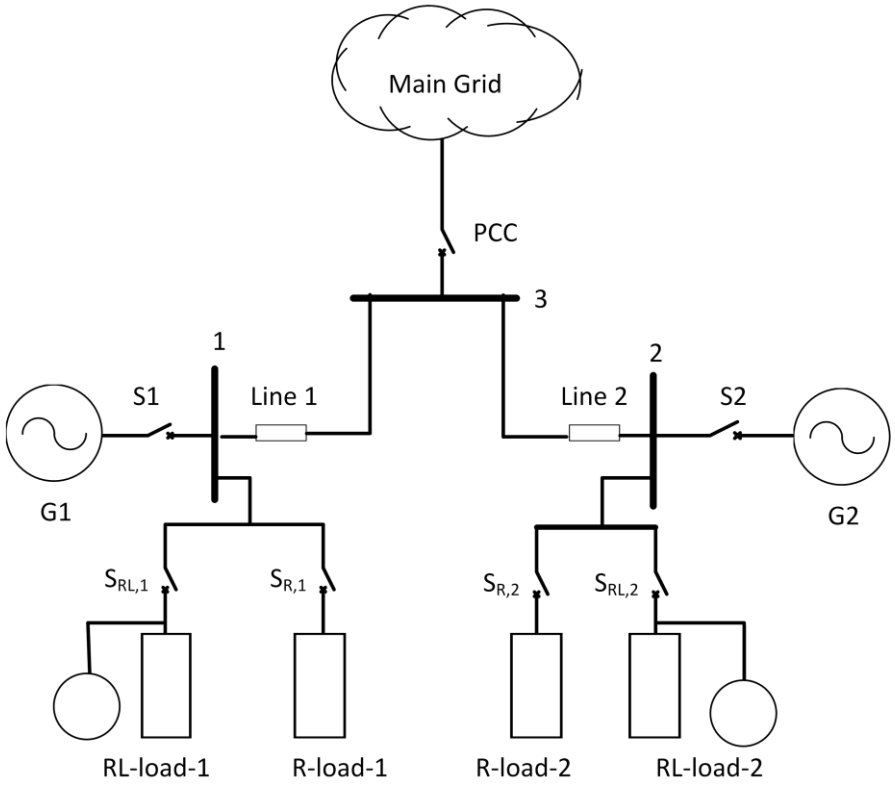

Figure 5.1. The laboratory microgrid system

A computer equipped with LabVIEW® software and NI PCI 6221 data acquisition card acts as a local controller which commands torque and field voltage to the DC machine drive and the power supply respectively. The rating of various pieces of equipment is listed in Table 5.1.

Table 5.1 Laboratory equipment ratings

Equipment	Parameter	Rating	Units
Synchronous Machine	Voltage	230/460	Volts
	Current	6.28/3.14	Amps
	Power	2.5	kVA
	Power Factor	0.8	lagging
	Field Voltage	150	Volts
	Field Current	1.05	Amps
DC Machine	Voltage	240	Volts
	Current	70.5	Amps
	Power	20	HP
	Field Voltage	150	Volts
	Field Current	2.7/1.3	Amps
	Speed	1750/2700	Rpm
DC Machine Drive	Input Voltage	3-230...500	Volts
	Input Current	114	Amps
	Input frequency	50-60	Hz
	Output Voltage	240...500	Volts
	Output Current	140	Amps
	Field Current	6	Amps
Programmable DC power supply	Input Voltage	115-230	Volts
	Input Current	11/6	Amps
	Input Phases	1	Phase
	Input Frequency	50-60	Hz
	Output Voltage	0-300	Volts
	Output Current	0-2	Amps

5.2. MICROSOURCES

A block diagram of the generating units is shown in Figure 5.2. Each generating unit is a three-phase synchronous machine. The shaft of the synchronous machine is coupled to that of a DC machine. The DC machine represents a prime mover like an engine. The torque applied by the DC machine on the shaft is analogous to the fuel valve opening in an engine. The DC machine is controlled by a Saftronics DC400 drive. The drive is responsible for producing field and armature currents required by the machine to ensure that the commanded torque τ^* is applied to the shaft by the DC machine. The field winding of the synchronous machine is supplied by a Sorensen programmable power supply which emulates an exciter. The power supply is responsible for supplying the commanded field voltage to the field winding of the synchronous machine. Both the Saftronics DC400 drive and the Sorensen programmable power supply are controlled by the MC over Ethernet.

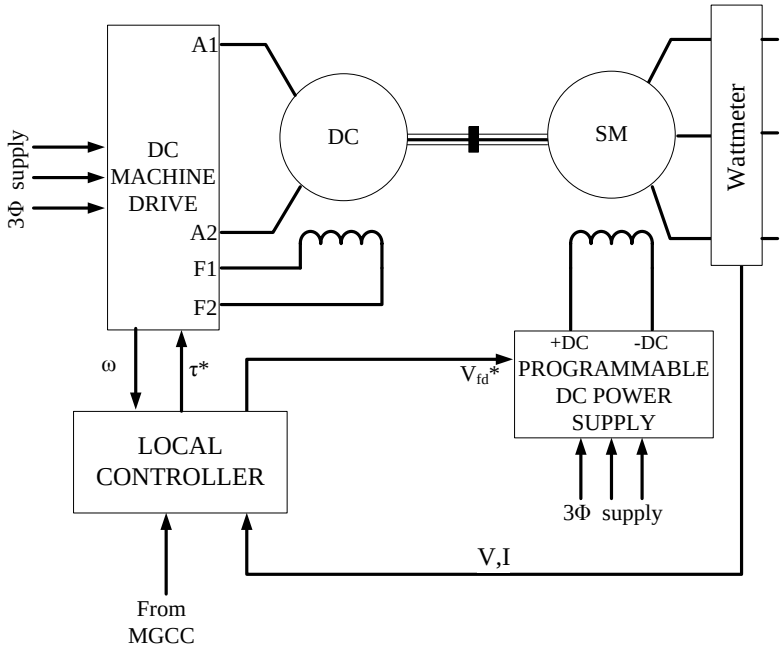

Figure 5.2. Generating Unit Line Diagram

The wattmeter comprises of three LEM LV 25-P potential transformers and three LEM LA 55-P current transducers mounted on each phase. These currents and voltages sensors are connected to the PCI 6221 DAQ's analog input ports. The frequency and active and reactive powers are calculated in the MC.

5.3. LOADS

Resistive and Resistive-Inductive loads have been used as active and reactive power loads in the microgrid. As shown in Figure 5.3, resistive loads comprise of three 100 Ω resistors connected in star. Induction machines at no-load are used as reactive power loads in the system. The resistive-inductive loads comprise of a resistive load in parallel with an induction machine. Two different types of induction machines IM1 and IM2 are used in the system. Table 5.2 details the ratings of the equipment used for loads. Each resistive load bank draws 506.25W (approx. 500W) at rated voltage. IM1 and IM2 draw approximately 500VAR and 2000VAR respectively at rated voltage.

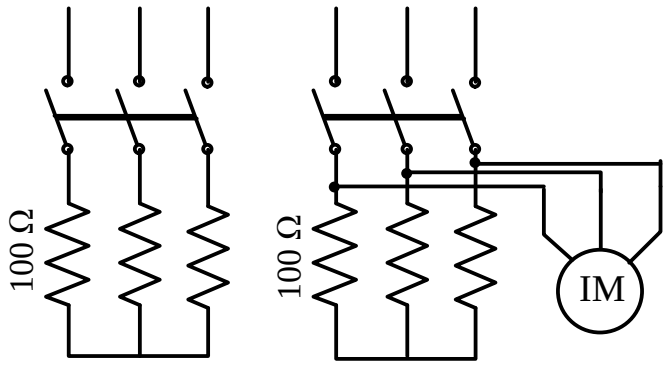

Figure 5.3 Resistive and Resistive-Inductive load banks

Table 5.2 Load equipment ratings

Equipment	Parameter	Rating	Units
Load Resistor	Resistance	100	Ohms
	Power	225	Watts
Load IM- I	Voltage	230/460	Volts
	Current	2.9/1.5	Amps
	Speed	1735	Rpm
	Frequency	60	Hz
	Power	0.75	HP
Load IM- II	Voltage	230/460	Volts
	Current	12.8/8.4	Amps
	Speed	1745	Rpm
	Frequency	60	Hz
	Power	5	HP

Buses 1 and 2 are equipped with loads: RL-load-1, RL-load-2, R-Load-1, and R-Load-2. Each of these loads comprise of several resistive and resistive-inductive loads as shown in the one-line diagram, Figure 5.4. Table 5.3 lists the calculation of the total active and reactive power drawn by each of these loads when all the switches are turned on.

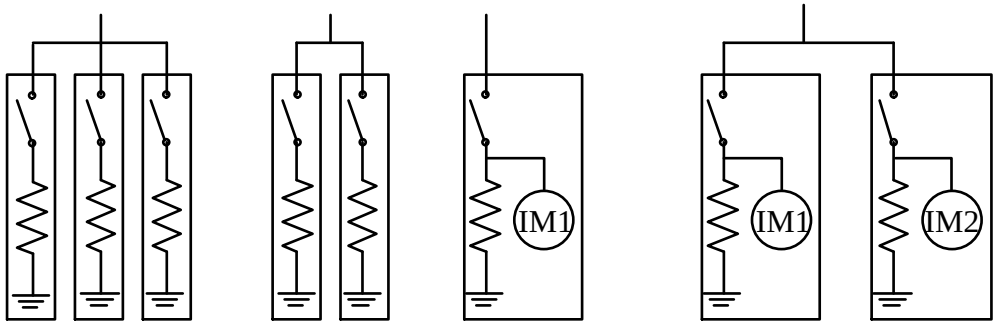

(a) R-load-1 (b) R-load-2 (c) RL-load-1 (d) RL-load-2

Figure 5.4 One-line diagram of the loads in the microgrid

Table 5.3 Loads in the microgrid

Load	No. of resistive load banks	No. of resistive-inductive load banks with IM1	No. of resistive-inductive load banks with IM2	Total active power demand (W)	Total reactive power demand (VAR)
R-load-1	3	0	0	1500	0
RL-load-1	1	1	0	500	500
R-load-2	2	0	0	1000	0
RL-load-2	2	1	1	1000	2500
Total	**8**	**2**	**1**	**4000**	**3000**

5.4. LINES

Buses 1 and 2 are connected to the point of common coupling with cables. These cables replicate the distribution lines between different points on a distribution network. AWG 12 cables are used for the laboratory setup. 153 feet of cable is used between buses 1 and 3 and 156 feet of cable is used between buses 2 and 3. The resistance of the cables was measured to be 243mΩ and 248mΩ between buses 1 and 3 and buses 2 and 3 respectively.

6. TEST RESULTS

6.1. MICROGRID OPERATING PROCEDURE

6.1.1. Startup. Initially, it is assumed that the loads within the area of the microgrid are being served by the grid and the DGs are installed within the microgrid and are ready to be started. Every DG is assumed to have a switch/breaker which connects it to a bus within the microgrid. Initially the switch is assumed to be open. The objective of the startup procedure is to get the DGs started and ready to supply power to the network when needed.

The following procedure is suggested:

1. Start the prime movers (DC machines in our case) of the synchronous machines.
2. Bring up the speed to 1800 rpm (corresponding to 60 Hz frequency of the grid). This can be done by running the DG in droop mode. Since the DG is not connected to the microgrid, the load being served is zero. At no load the DG will run at 1800 rpm based on the droop characteristics.
3. Apply field voltage such that it is very close to the voltage of the bus to which it is being connected.
4. The synchronization lamps should be blinking very slowing. Close the contactor at an instant when all the lamps are off.
5. Switch the DG into constant power mode.

6.1.2. Unintentional Islanding. This is a situation when there is a fault, and the grid is unable to supply power to the microgrid. Synchronous machine based DGs can be very valuable in such situations. It is very important that the grid supply be monitored at all times and once the MGCC decides to island, all the MCs are instructed to switch to droop mode. Figure 6.1 shows the system behavior during an unintentional islanding test case. The test procedure is described in Table 6.1.

The following observations can be made from these results.

- From Figure 6.1 (a) and (b) it is observed that the loads are always served at nominal voltage and frequency.
- From Figure 6.1 (c) and (d), once the both generators are commanded to supply power, power drawn from the grid decreases. When the system is connected to grid, the generators participate in serving the load.
- From Figure 6.1 (c) and (d), both generators DG1 and DG2 generate active and reactive powers as demanded by the system. The generators do not lose synchronism and both generators contribute to the power demanded by the system. Thus, the system maintains stability during all modes of operation.
- At t=145 sec and t=180 sec, the load in the system is changed. This change in load results in voltage and frequency transients. It can be noticed that the size of the transient corresponds to the size of load being added. When R-load-1 was added at t=145sec, there is a very small voltage transient since there is no considerable amount of reactive load added to the system. But at t=180sec, when RL-load-2 is added, the voltage transient is much larger. Similar transients can be observed on the system frequency.

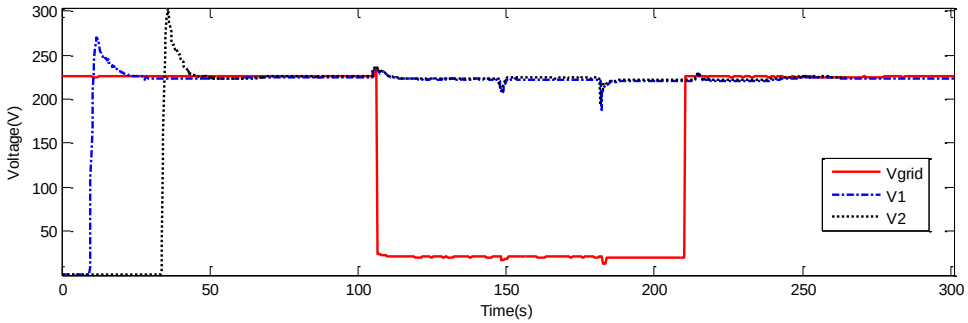

(a) Voltage at buses 1(V1), 2(V2) and 3(Vgrid)

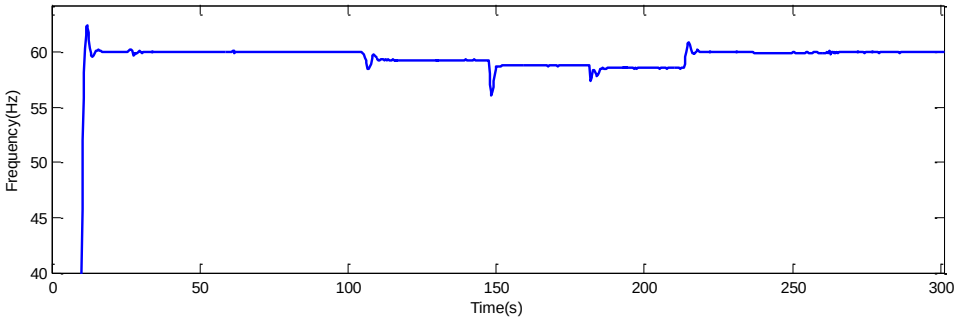

(b) System frequency as calculated from the speed of DG1

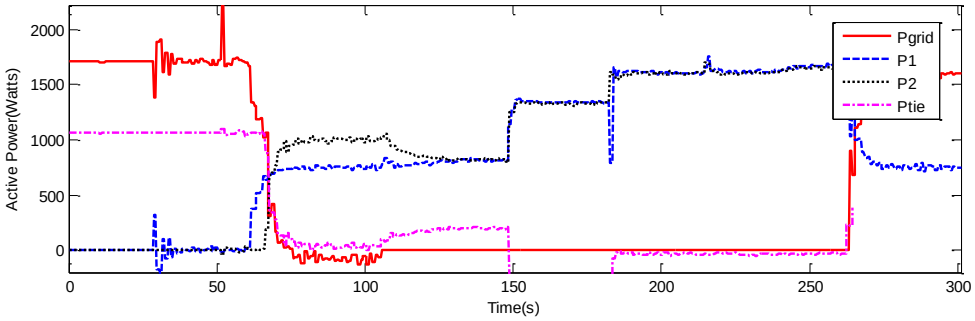

(c) Active power flows from DG1(P1), DG2(P2) and grid(Pgrid) and that into bus 2 (Ptie)

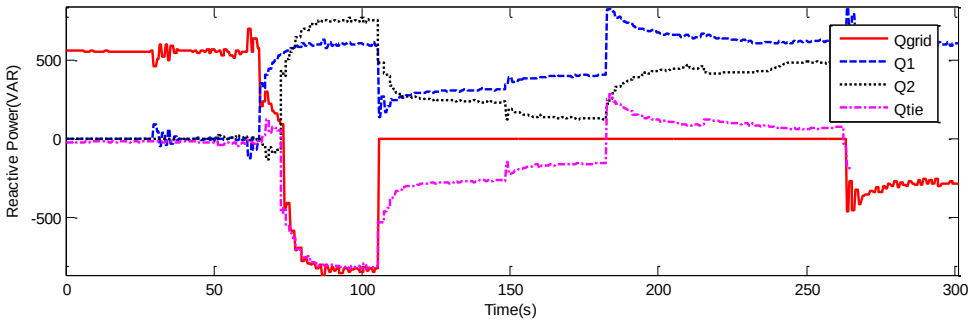

(d) Reactive power flows from DG1(Q1), DG2(Q2) and grid(Qgrid) and that into bus 2 (Qtie)

Figure 6.1. System behavior during unintentional islanding

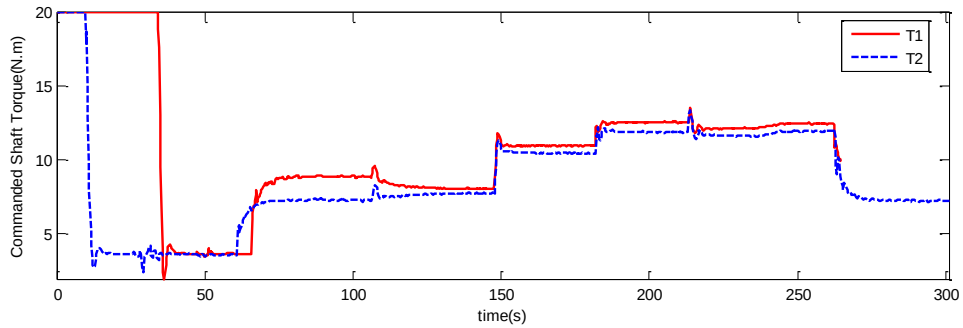

(e) Torque commanded to DG1(T1) and DG2(T2)

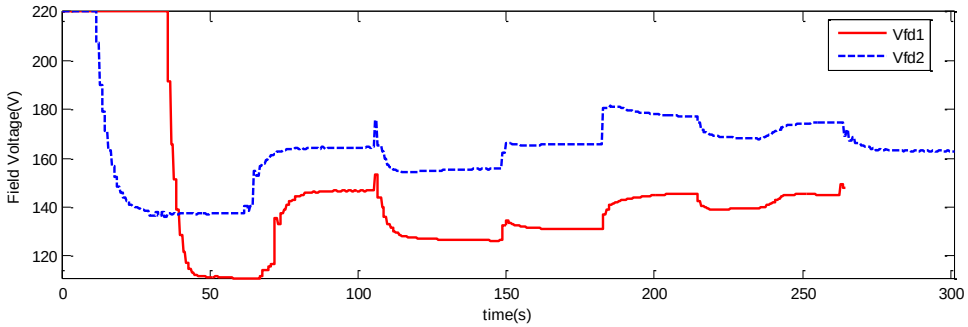

(f) Field voltage applied to DG1(Vfd1) and DG2(Vfd2)

Figure 6.1. System behavior during unintentional islanding, cont'd.

Table 6.1 Unintentional islanding procedure

Time(sec)	Event
0	Grid is serving a total load of P=1700 W, Q=500 Var. G1 and G2 are off. S1 and S2 are open.
10	G1 is turned on and brought up to speed and synchronized with bus 1.
50	G2 is turned on and brought up to speed and synchronized with bus 2.
60	G1 is commanded to supply 750 W and 600 Var each.
65	G2 is commanded to supply 1000 W and 650 Var each.
110	Grid voltage is too low. System is islanded.
145	R load is added on station 1
180	RL load is added on station 6
220	Grid voltage is again within acceptable range
275	Microgrid PCC is synchronized with the grid and PCC breaker is closed

6.1.3. Intentional Islanding. This is a situation when it is decided, a priori, that the microgrid has to go into islanded mode and there is sufficient time to perform intentional islanding. One of the possible reasons for this situation can be when the power quality of the grid is poor and it is decided to switch to islanded mode.

The primary objective is to keep the voltage and frequency dip to a minimum during transition from grid-connected mode to islanded mode. Thus the following procedure is suggested:

1. Shed loads which are beyond the total generating capacity of all DGs in the microgrid. Load shedding can be based on the priority of the load.
2. At the instant after islanding, the power shortage within the microgrid is equivalent to the amount that the grid was serving before islanding. Thus, based on machine capabilities and economic considerations, increase generation at some or all of the DGs in the microgrid such that the power from the grid is negligible.
3. As soon as the power drawn from the grid is negligible, the point of common coupling for the microgrid can be disconnected and all the machines are switched to droop mode by the MGCC.

In case of intentional islanding, at the time the point of common coupling is disconnected from the utility grid, there is no power being drawn from the grid. Hence the voltage and frequency transients are much smaller when compared to the case of unintentional islanding. Figure 6.2 and Figure 6.3 compare the voltage and frequency dip during islanding for both intentional and unintentional islanding situations. Hence the voltage dip is 4.6 V (2.04%) in the case of intentional islanding as against 33.5 V (14.8%) during unintentional islanding. The frequency dip is 1.65 Hz (2.75%) during intentional islanding versus 4.9 Hz (8.16%) during unintentional islanding.

6.2. FACTORS AFFECTING MICROGRID PERFORMANCE

Various parameters affect the performance of the microgrid. Microgrids can be operated in series and parallel configurations [3]. Microgrid performance can be affected by the physical dimensions of the microgrid. Physical dimensions of the microgrid affect the length of the lines between the DGs. Power flows can be affected by the droop settings of the DGs as well. A study is performed to analyze the effect of pre-esisting levels of power flows in grid connected mode on system performance under islanded mode of operation. The effect of adding and removing large loads on the system is also performed.

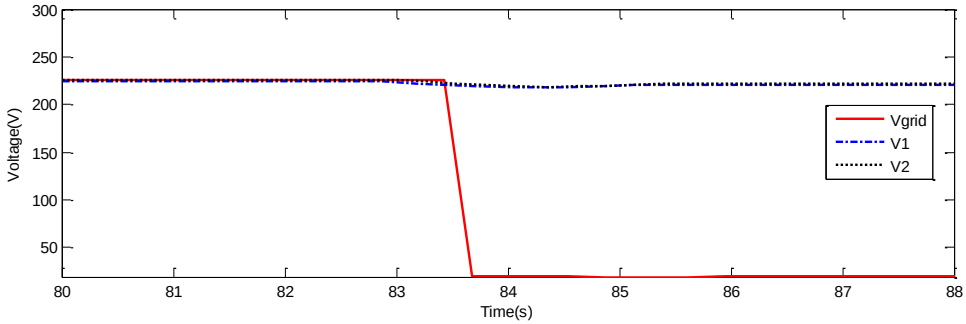

(a) Voltages at buses 1,2 and 3 during intentional islanding

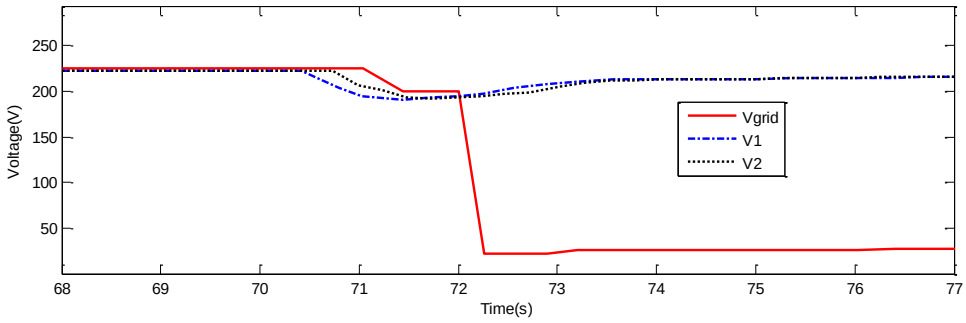

(b) Voltages at buses 1,2 and 3 during unintentional islanding

Figure 6.2 Voltage transient during islanding

6.2.1. Effect of Microgrid Architecture. Two architectures for microgrids, namely parallel and series have been studied for two machine microgrids. When all the DGs are connected to the point of common coupling, the architecture is known as parallel configuration. When all the buses are radially positioned with the point of common coupling, the architecture is known as series configuration. Figure 6.4 shows a one-line diagram for the parallel configuration and series configurations.

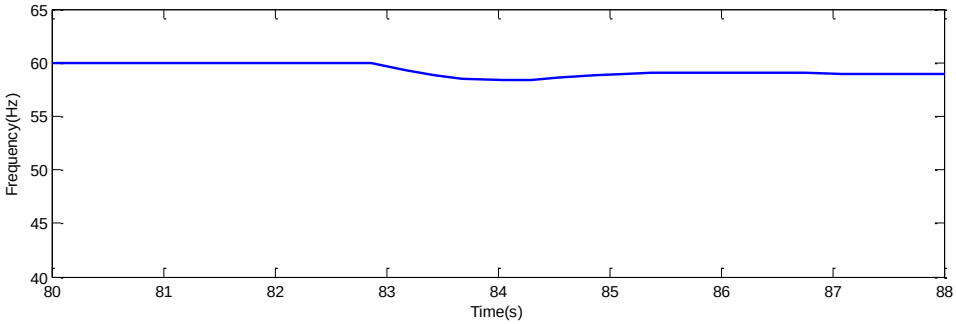

(a) System frequency during intentional islanding

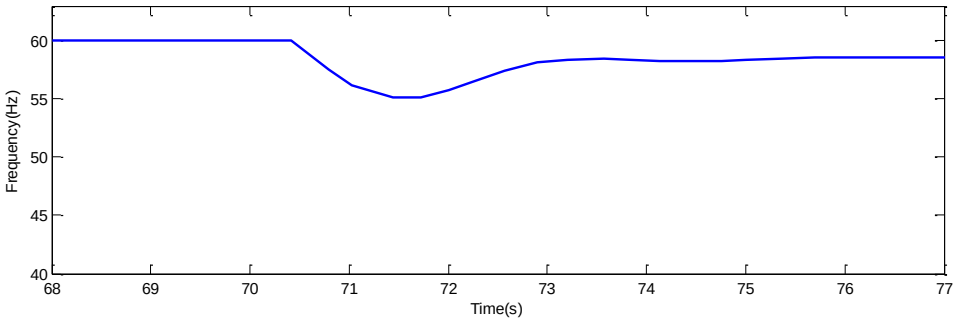

(b) System frequency during unintentional islanding

Figure 6.3 Frequency transient during islanding

The following points are worth noting in regard to the architectures:

1. In a two DG microgrid system, the positioning of the grid affects the architecture. If the grid is connected directly to one of the buses then it is a series configuration. If it is connected between the DGs then it is parallel.
2. If the grid is connected to one of the buses in the system, the bus voltage will remain stiff during grid-connected mode. Hence given a choice the grid can be connected to a bus serving any voltage sensitive equipment.
3. In the islanded mode, there is no difference between the configurations.

Figure 6.5 and Figure 6.6 show the similar test results for series and parallel microgrids. The series microgrid is islanded at t=50sec. Grid voltage is back up at t=115sec and the microgrid is reconnected at t=125sec. The parallel microgrid is islanded at t=125sec. Grid voltage is back up at t=95sec and the microgrid is reconnected at t=135sec. During grid connected mode it can be noticed that both DGs are operating at the same voltage in the case of parallel microgrid but in case of series microgrid there is a voltage drop between DG1 and DG2. But this does not affect the voltage or the power flows during islanded mode.

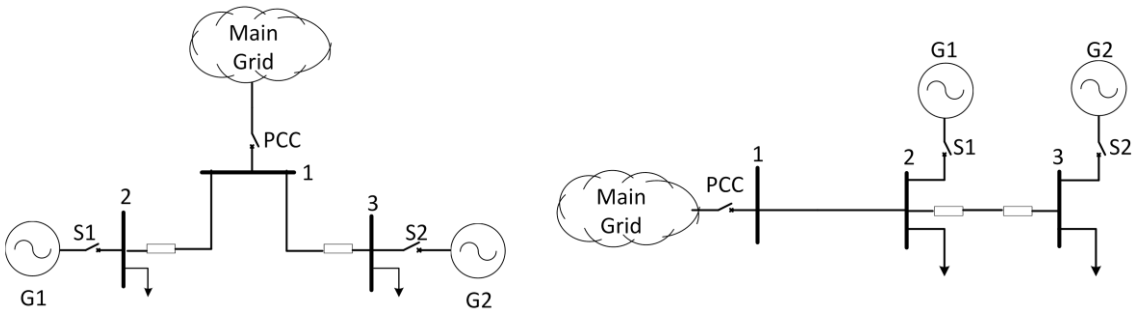

(a) Parallel configuration (b) Series Configuration

Figure 6.4. Microgrid architecture

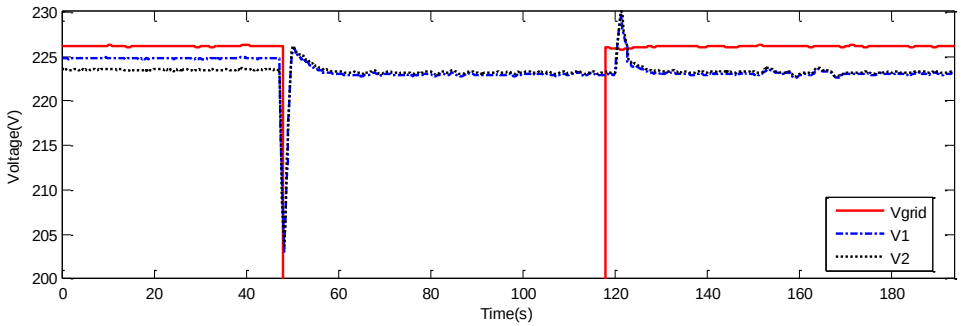

(a) Voltage at buses 1(V1), 2(V2) and 3(Vgrid)

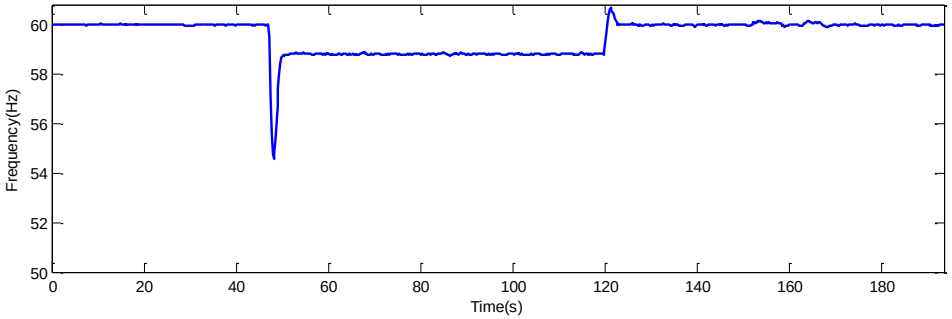

(b) System frequency as calculated from the speed of DG1

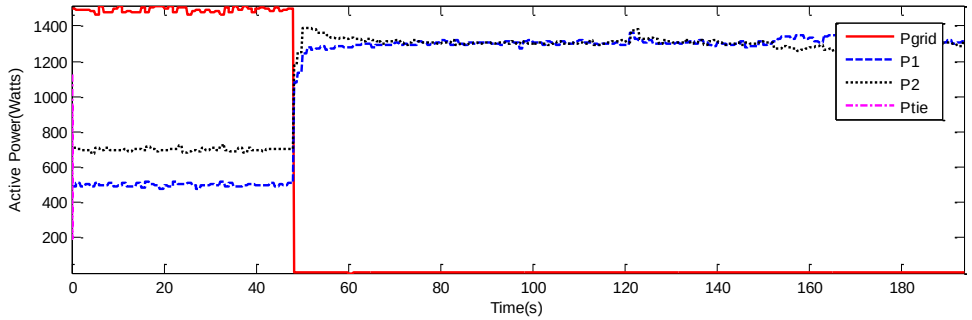

(c) Active power flows from DG1(P1), DG2(P2) and grid(Pgrid) and that into bus 2 (Ptie)

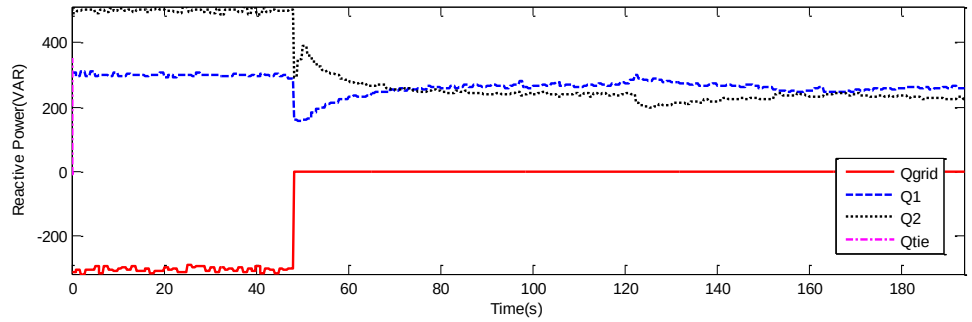

(d) Reactive power flows from DG1(Q1), DG2(Q2) and grid(Qgrid) and that into bus 2 (Qtie)

Figure 6.5 Series microgrid system behavior

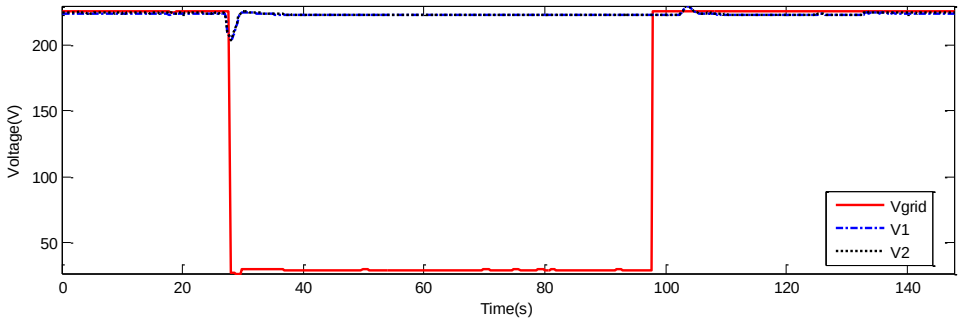

(a) Voltage at buses 1(V1), 2(V2) and 3(Vgrid)

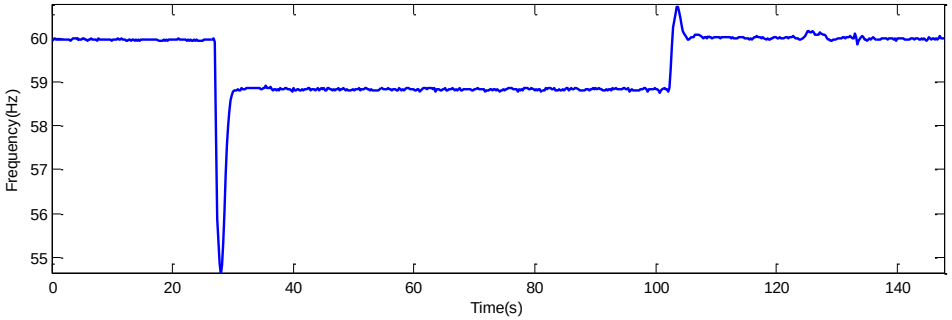

(b) System frequency as calculated from the speed of DG1

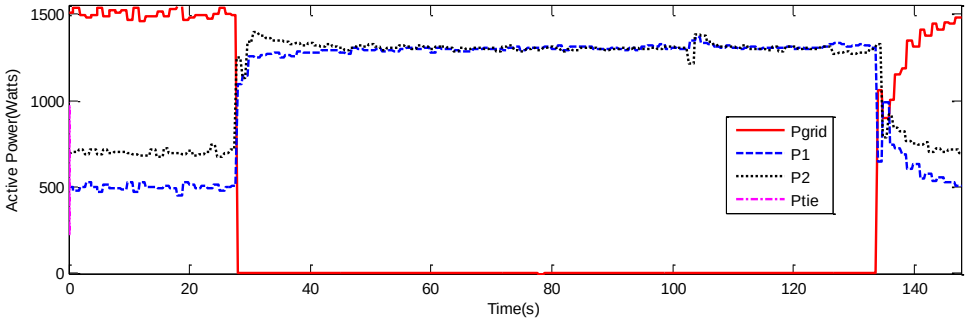

(c) Active power flows from DG1(P1), DG2(P2) and grid(Pgrid) and that into bus 2 (Ptie)

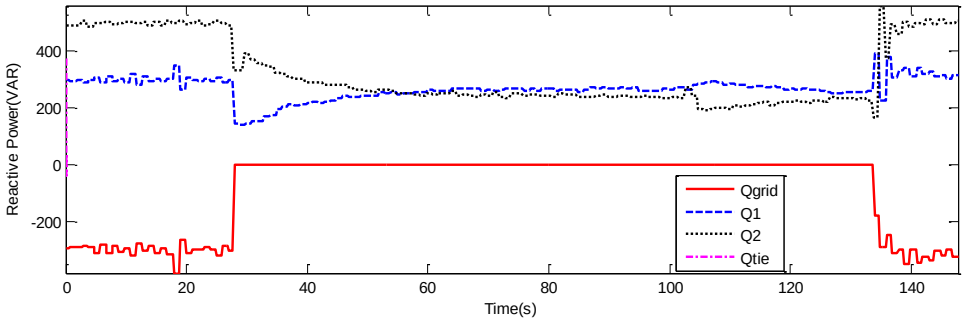

(d) Reactive power flows from DG1(Q1), DG2(Q2) and grid(Qgrid) and that into bus 2 (Qtie)

Figure 6.6 Parallel microgrid system behavior

6.2.2. Effect of Line Impedance. The length of the lines connecting the DGs to the PCC determines the impedance between them. During grid connected mode, this impedance affects the voltage at the DGs. For longer line lengths, the impedance between the PCC and the DG is large enough causing the voltage to drop significantly. Since the reactive power depends on the voltage in the droop mode, line impedance can affect the reactive power sharing between the DGs. Figure 6.7 shows the reactive power and voltage waveforms when there is no cable connected between the DGs and the PCC. At t=60sec, the system is islanded. V1 is slightly lower than V2 in islanded mode and as a result, DG1 generates a higher share of reactive power in comparison to DG2. Reactive power share is very sensitive to the voltage. For a 5% droop, reactive power generated increases at a rate of 133.33 Var for a 1V drop in voltage.

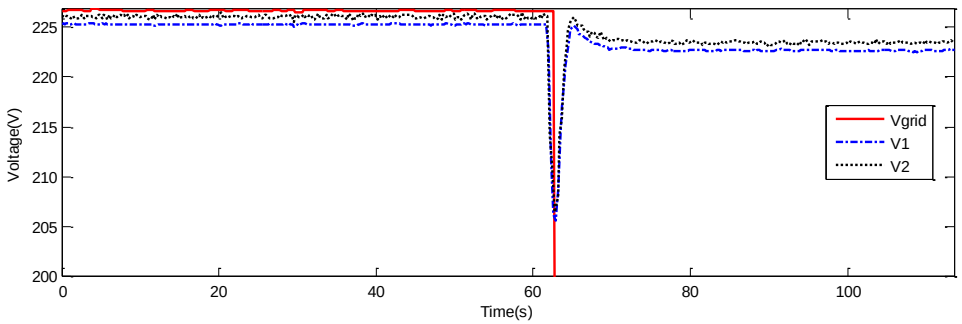

(a) Voltage at buses 1,2 and 3 for the test without line impedance

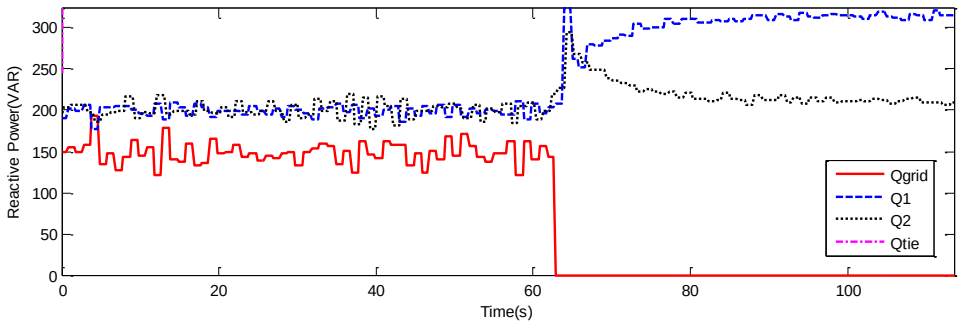

(b) Reactive power flows for the test without line impedance

Figure 6.7 System behavior without line impedance

Figure 6.8 shows the reactive power and frequency waveforms for a system with all the cable (300 feet) between buses 2 and 3. As a result of the impedance of the cable (490mΩ), the voltage at Bus 2 drops below the voltage at Bus 1. At t=40sec, the system is islanded. Thus the reactive power generated by DG2 is higher than that generated by DG1 during islanded mode.

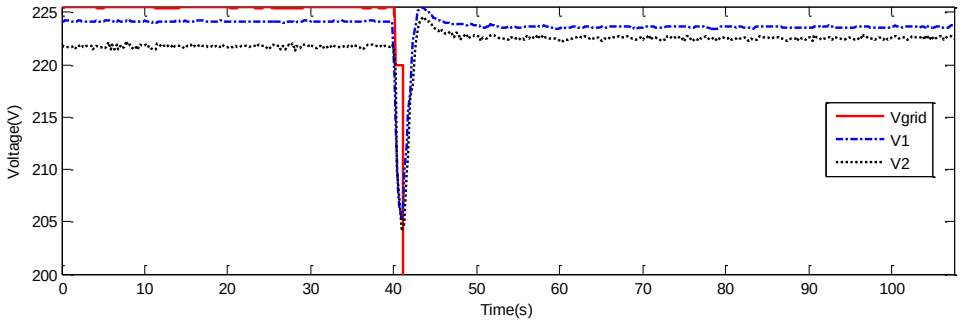

(a) Voltage at buses 1,2 and 3 for the test with line impedance

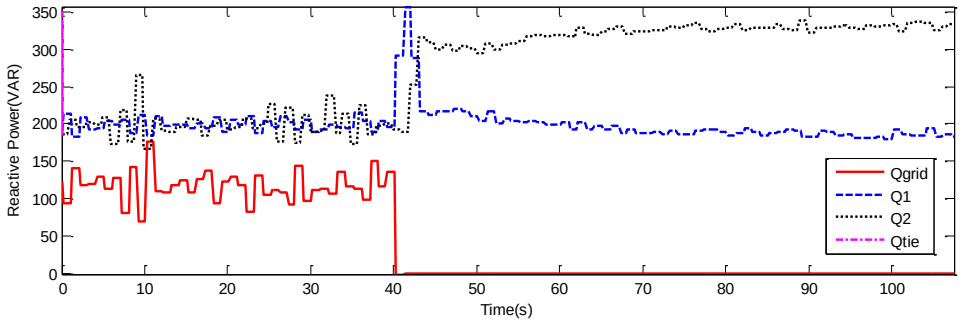

(b) Reactive power flows for the test with line impedance

Figure 6.8 System behavior with line impedance

6.2.3. Effect of Droop Setting. Droop settings impact the share of power being generated by a generating station. Higher droop percentages will result in steep droop characteristics decreasing the share of power generated by the DG. Figure 6.9 shows the frequency and active power waveforms for a system operating on different active power-frequency droop percentages. DG1 is operating on 3% droop and DG2 is operating on 5% droop. As a result, DG1 generates more active power than DG2 during islanded mode. Hence, the active power generated by DG1 exceeds that of DG2 after the system is islanded at t=37sec.

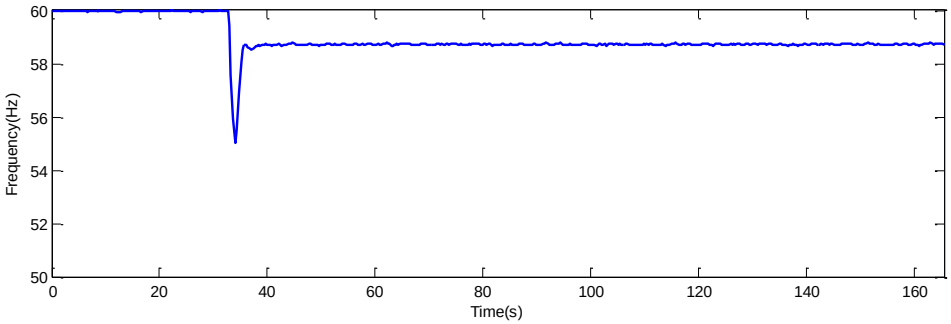

(a) System frequency as calculated from the speed of DG1

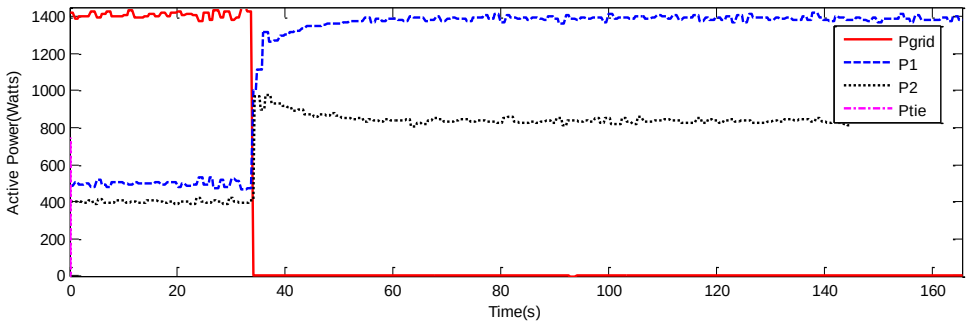

(b) Active power flow measurements from DG1, DG2, grid and tie line

Figure 6.9 Frequency and active power waveforms for DGs operating on different active power - frequency droop percentages

Figure 6.10 shows the reactive power and voltage waveforms when DG1 is operating on a 5% reactive power droop and DG2 is operating on a 3% reactive power droop. It can be observed that DG2 generates more reactive power. Hence, the reactive power generated by DG2 exceeds that of DG1 after the system is islanded at t=37sec.

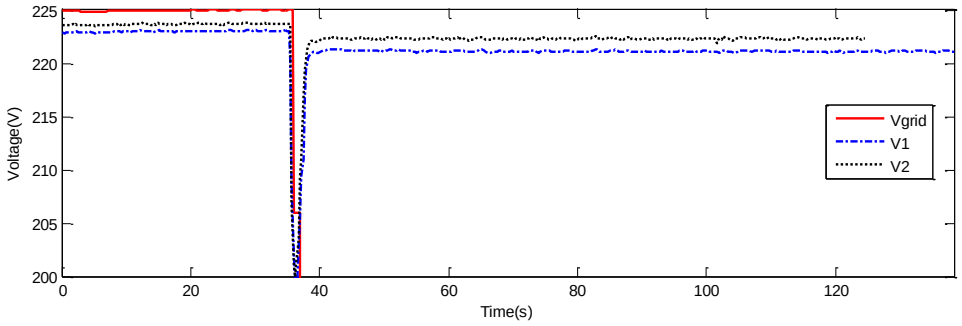

(a) Voltage at buses 1,2 and 3

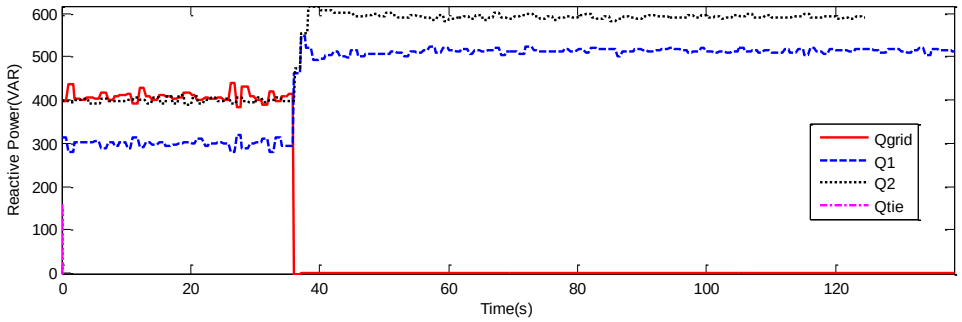

(b) Reactive power flows measurements from DG1, DG2, grid and tie line

Figure 6.10 Frequency and active power waveforms for DGs operating on different reactive power - voltage droop percentages

6.2.4. Effect of Grid Connected Generation on Droop Mode Power Sharing.

When the microgrid transitions from grid connected mode to islanded mode, MC changes from constant power mode to droop mode. Depending on how much power was commanded from the DGs in the system, the output active and reactive powers can have a sudden increase or a decrease. Four different tests are conducted on the microgrid system which are described below. In all the cases the load in the system is held constant

at 1500W and 500VAR measured at rated voltage. Since the load is constant impedance, the power consumed varies with voltage. The trajectory of the operating point is plotted on the droop curve for a period of 10 seconds around the time of islanding.

1. An unintentional islanding case when there is a power deficit in the system at the instant of islanding. Figure 6.11 (a) and (b) show the transition of DG1 and DG2 from grid connected to islanded mode during this case. Both DG1 and DG2 are generating 500 W and 500 VAR before islanding. After islanding the system stabilizes around 850W from both DG1 and DG2, and 960 Var from DG1 and 850 Var from DG2.

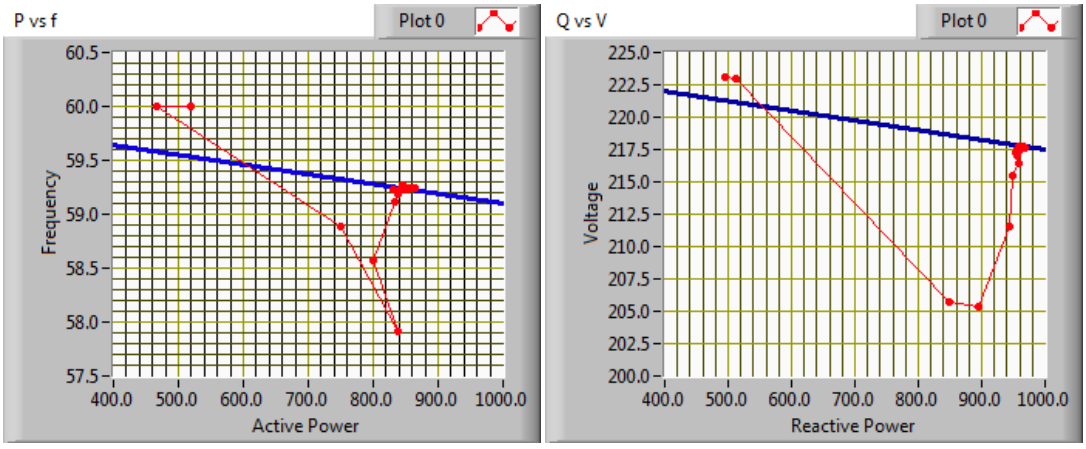

Figure 6.11 (a) DG1 transition to islanded mode for unintentional islanding with power deficit

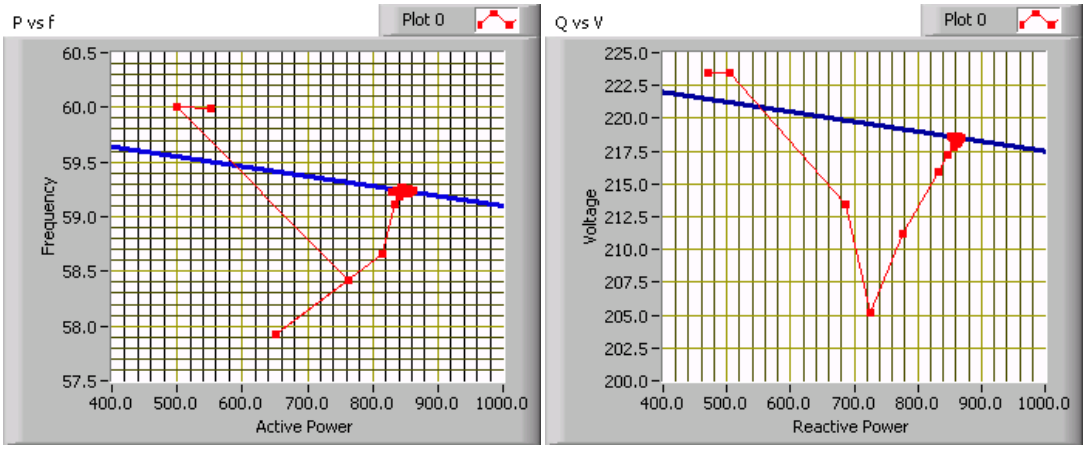

Figure 6.11 (b) DG2 transition to islanded mode for unintentional islanding with power deficit

2. An intentional islanding case when DG1 is generating 850 W and 950 Var and DG2 is generating 850 W and 850 VAR. Figure 6.12 (a) and (b) show the transition of DG1 and DG2 from grid connected to islanded mode during this case. Even in this case, after islanding the system stabilizes around 850 W from both DG1 and DG2, and 960 Var from DG1 and 850 Var from DG2.
3. An unintentional islanding case when there is excess power in the system at the instant of islanding. Figure 6.13 (a) and (b) show the transition of DG1 and DG2 from grid connected to islanded mode during this case. Both DG1

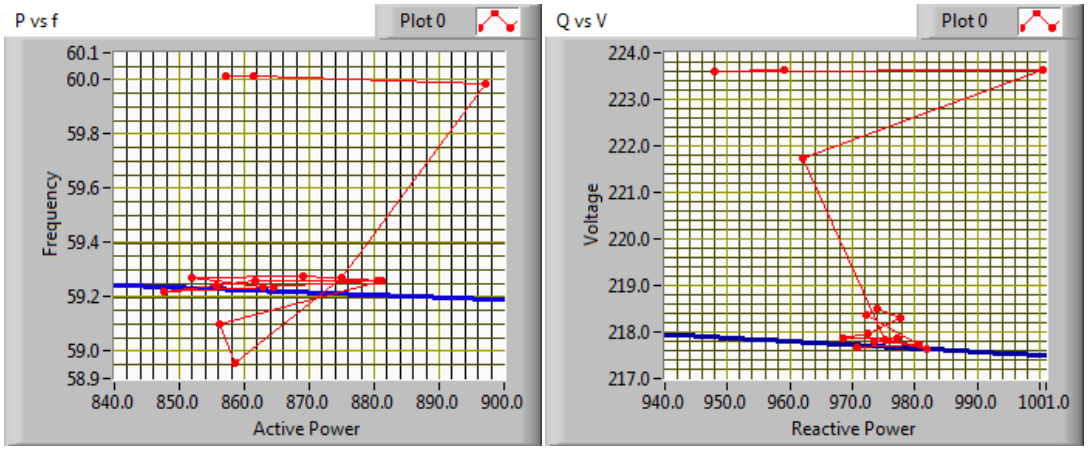

Figure 6.12 (a) DG1 transition to islanded mode for intentional islanding

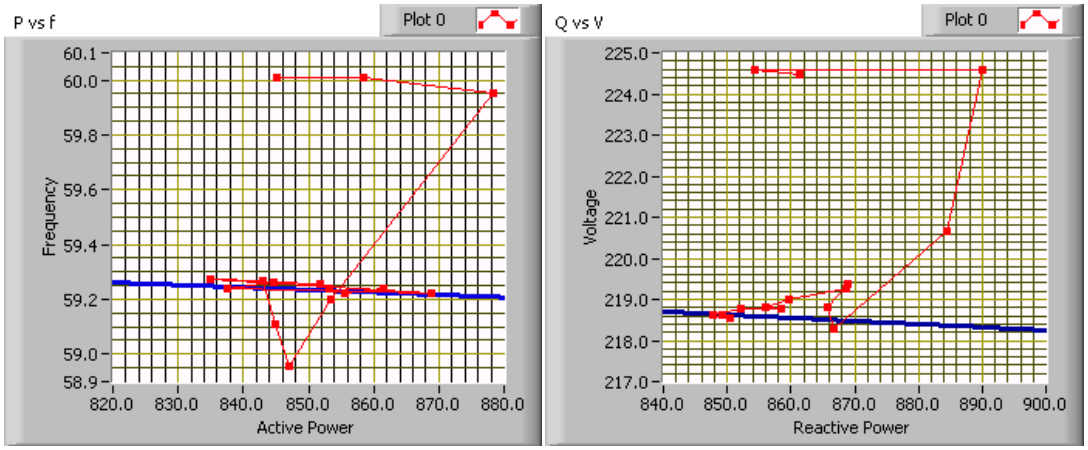

Figure 6.12 (b) DG2 transition to islanded mode for intentional islanding

and DG2 are generating 1500W and 1500VAR before islanding. Again, after islanding the system stabilizes around 850W from both DG1 and DG2, and 960 Var from DG1 and 850 Var from DG2.

4. An unintentional islanding case when the DG1 is generating more than its share of power and DG2 is generating less than its share of power. Figure 6.14 (a) and (b) show the transition of DG1 and DG2 from grid connected to islanded mode during this case.DG1 is generating 500W and 500VAR before

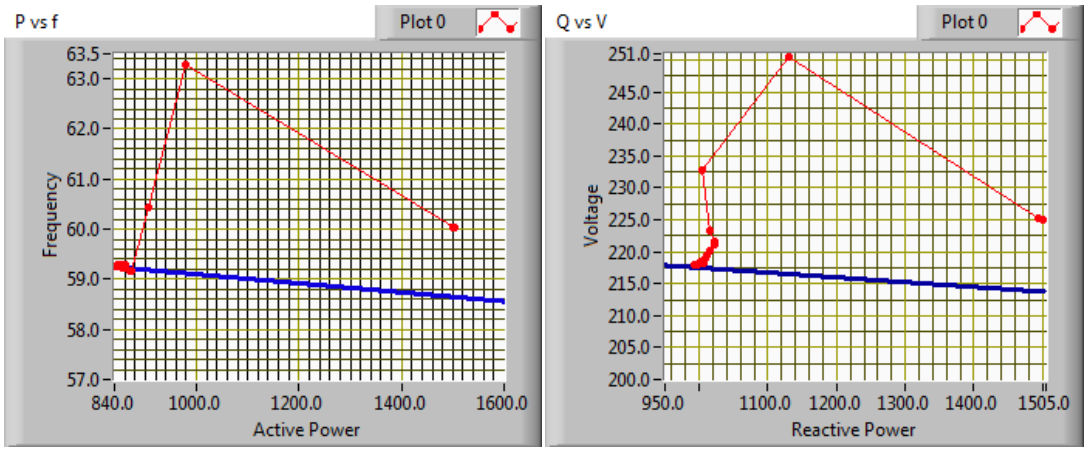

Figure 6.13 (a) DG1 transition to islanded mode for unintentional islanding with excess generation

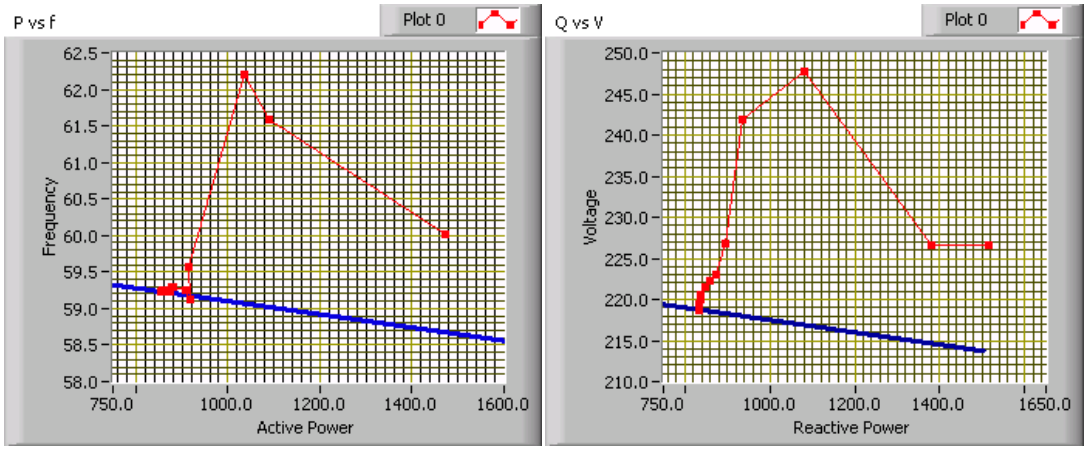

Figure 6.13 (b) DG2 transition to islanded mode for unintentional islanding with excess generation

islanding. Again in this case the after islanding, the system stabilizes around the same point as before.

These test can conclude that irrespective of the power generated during grid connected mode, the power sharing is not altered during islanded mode. The trajectory followed by the system depends on the PI gains of the controllers. A faster controller can result in a faster dynamic of the system.

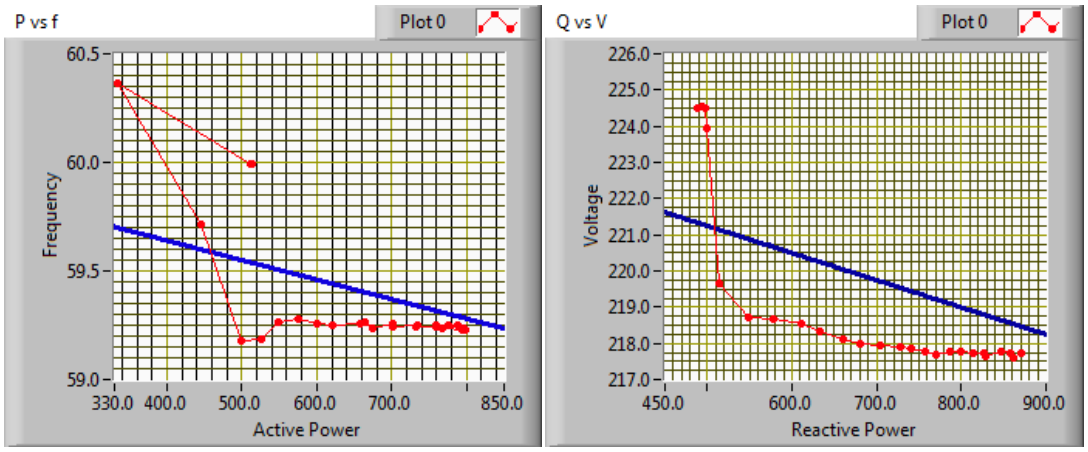

Figure 6.14 (a) DG1 transition to islanded mode with unequal generation

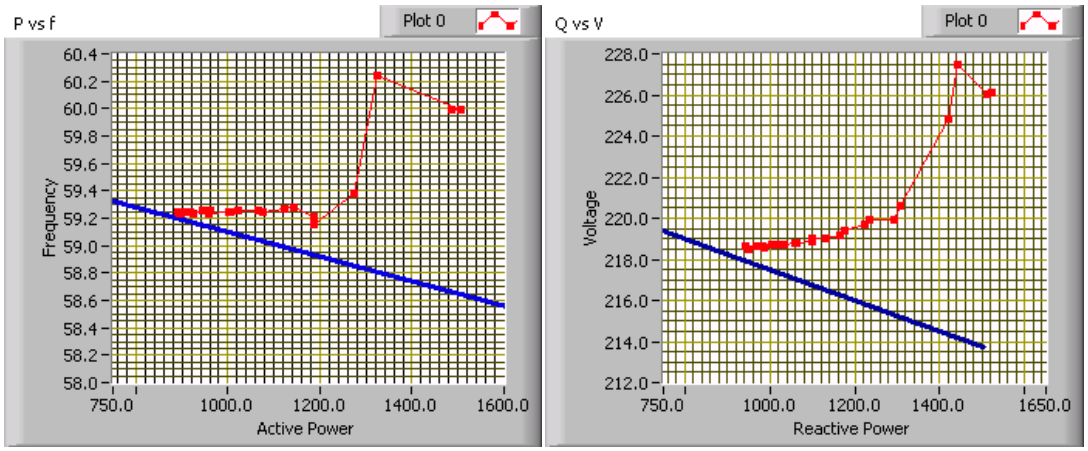

Figure 6.14 (b) DG2 transition to islanded mode with unequal generation

6.2.5. Effect of Heavy Loads on System Performance. During islanded mode, the system stability is maintained by the droop control. Droop control depends on active and reactive power. Small changes in load can have a drastic impact on the voltage and frequency. Figure 6.15 shows the system behavior during an extreme test when the system load is changed from 0% to 100% of the rated load instantaneously. The frequency and voltage drop below acceptable operating standards and will trigger any protection equipment in the system but it can be observed that even during this extreme case, the generators do not loose synchronism and the system is back to normal operating conditions in 4 seconds. This is possible only because of the inertia based synchronous machines in the system.

During normal operation of a microgrid system, the probability of a 4000W, 3000VAR load being turned on instantaneously in a 4000W, 3000VAR rated system is very small. As explained in Section 6.1.2, the size of the transient depends on the size of the load being added into the system. Thus this is the worst case transient. Since the system is able to recover from the worst case transient, the system can be considered stable for all transients. In reality the protection equipment would trip but in the laboratory setup since there is no protection equipment the test was conducted.

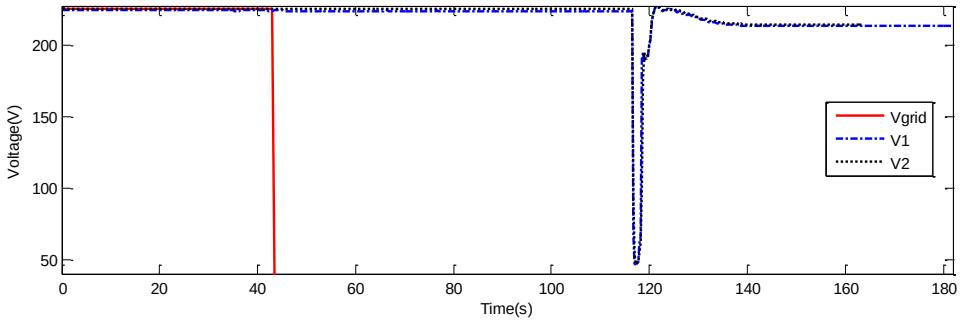

(a) Voltage at buses 1(V1), 2(V2) and 3(Vgrid)

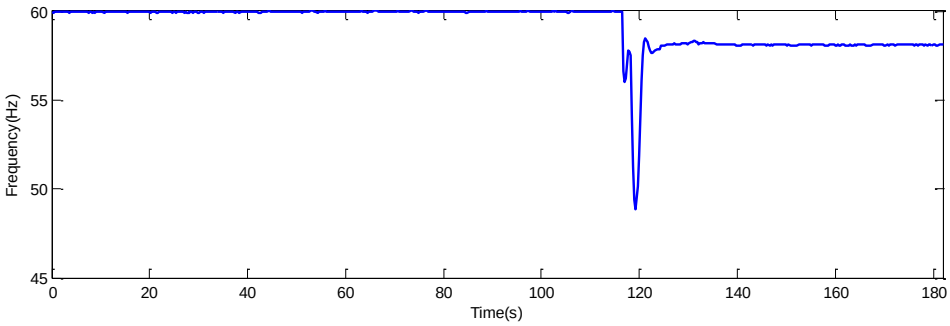

(b) System frequency as calculated from the speed of DG1

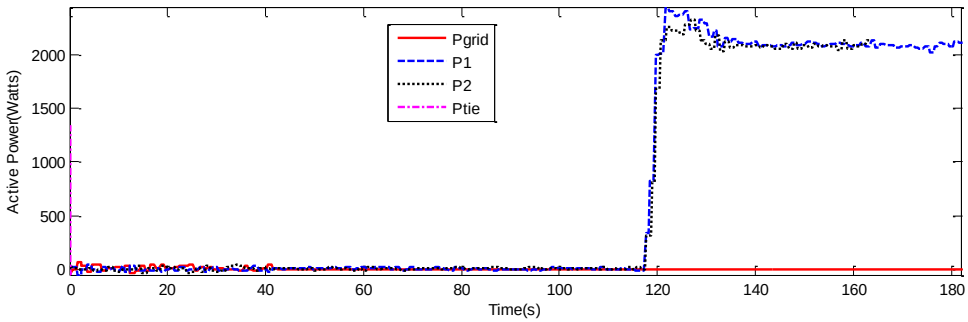

(c) Active power flows from DG1(P1), DG2(P2) and grid(Pgrid) and that into bus 2 (Ptie)

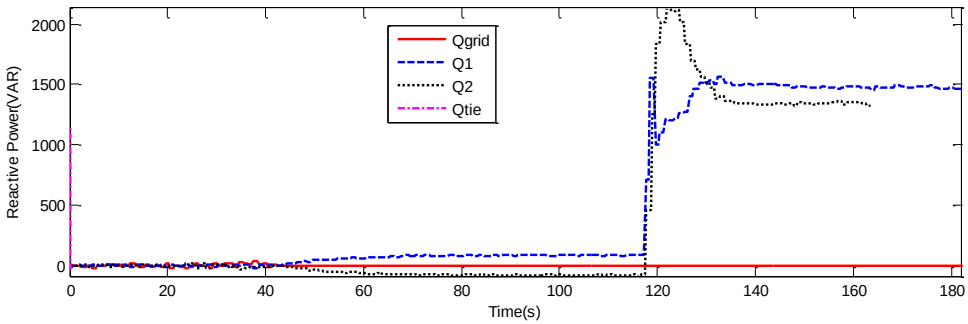

(d) Reactive power flows from DG1(Q1), DG2(Q2) and grid(Qgrid) and that into bus 2 (Qtie)

Figure 6.15 System behavior when load is changed from 0% to 100% of rated load

7. CONCLUSION AND FUTURE WORK

A laboratory test bench is created for testing microgrid operation and control schemes. A control scheme based on constant power mode and droop modes has been proposed for the operation of the microgrid. It has been demonstrated that the loads in the microgrid are served with nominal voltage and frequency with or without grid support while ensuring that the generating units are stable and share the load. Operating procedures for startup, unintentional islanding and intentional islanding have been proposed and demonstrated. The microgrid has been tested with series and parallel configurations, varied line lengths, and different droop settings. The impact of heavy loads suddenly being turned on has been studied and it is proven that the system will remain stable at all times.

In the future, the laboratory setting may be augmented with electronic loads and inverter based DGs. Battery banks can be connected to the system to help during large transients. There are various parameters involved in the control strategy such as droop percentage, no-load frequency and voltage which can be modified to suit the system requirements. Economic models can be incorporated into the selection of these parameters. Protection issues can be studied and suitable protection schemes can be incorporated into the microgrid.

APPENDIX A

LABORATORY EQUIPMENT

Figure A.1 Synchronous machine

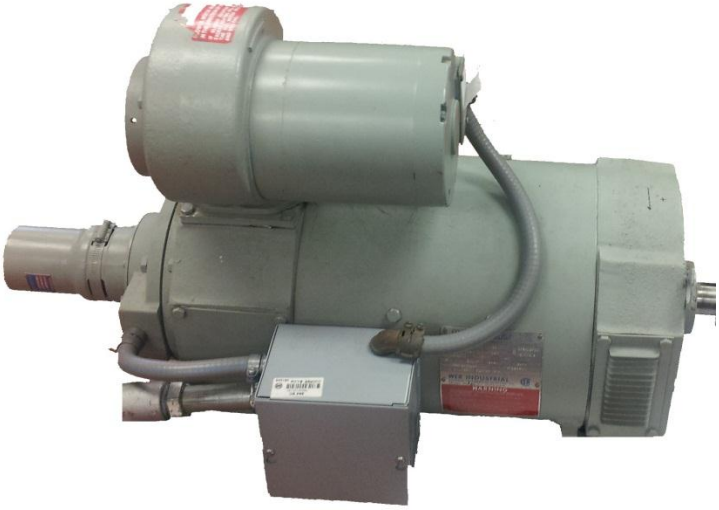

Figure A.2 DC machine (Prime-mover)

Figure A.3 DC machine drive

Figure A.4 Programmable Power Supply

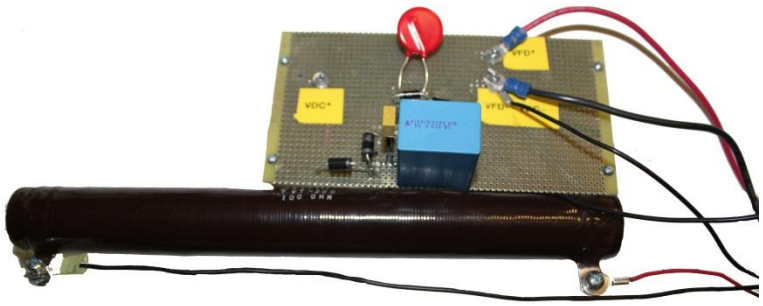

Figure A.5 Protection for field power supply

Figure A.6 Induction Machine – I Load

Figure A.7 Induction Machine – II Load

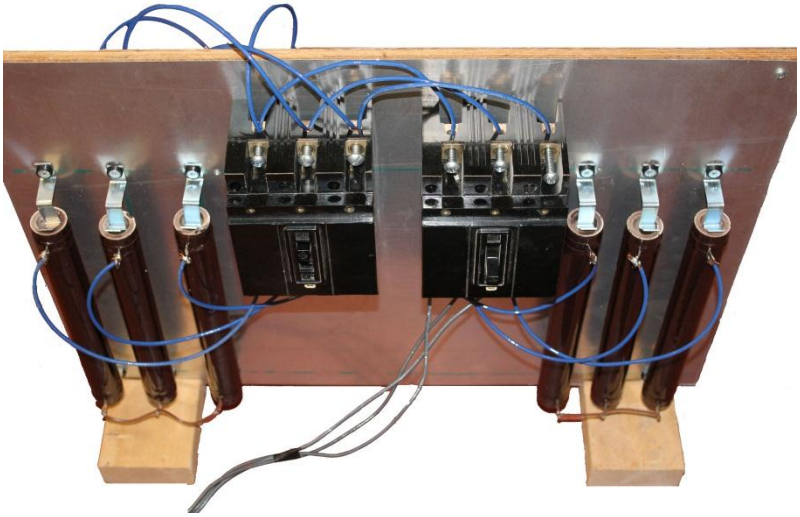

Figure A.8 Resistive load banks

Figure A.9 Synchronization lamps

APPENDIX B

LABORATORY WIRING DIAGRAMS

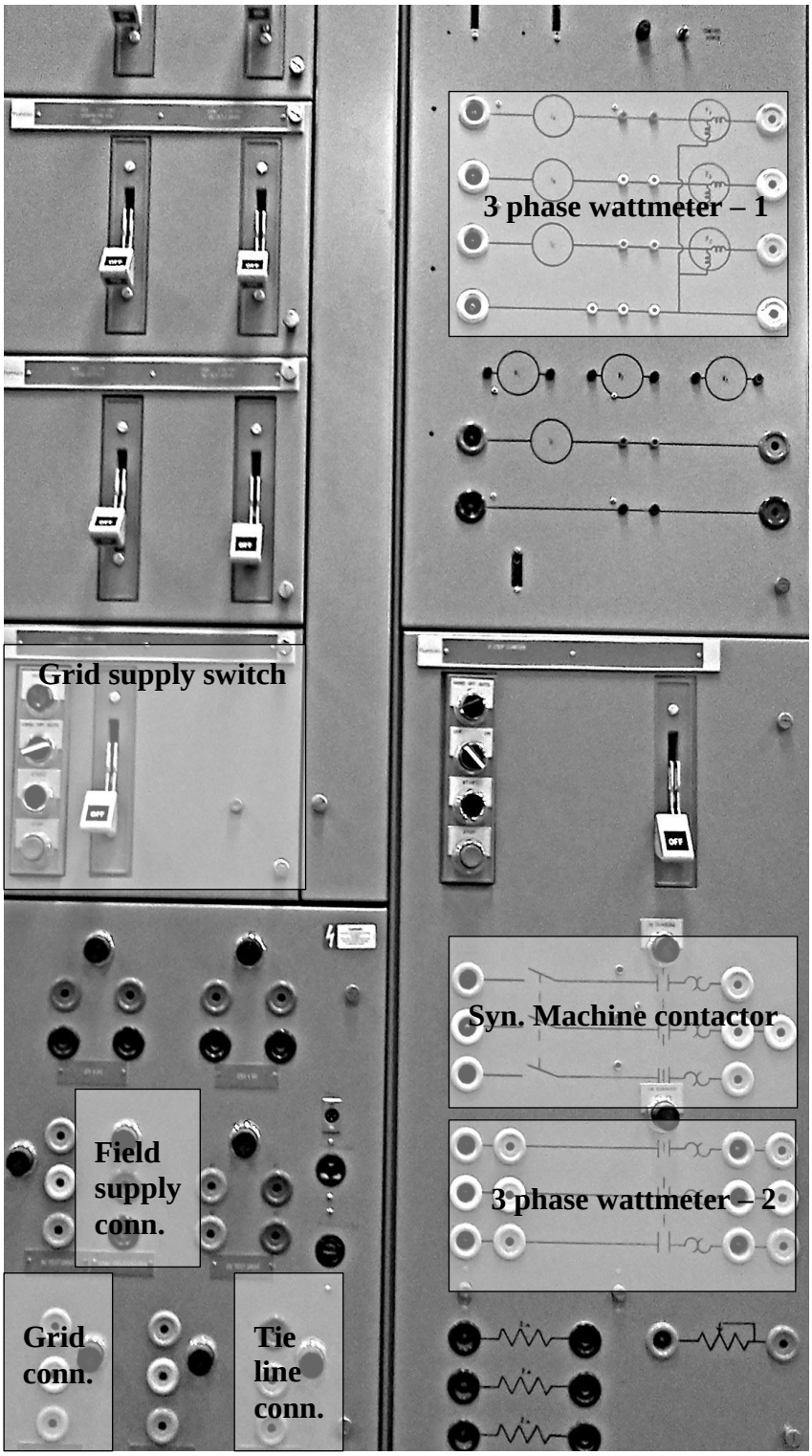

Figure B.1 Connection panel

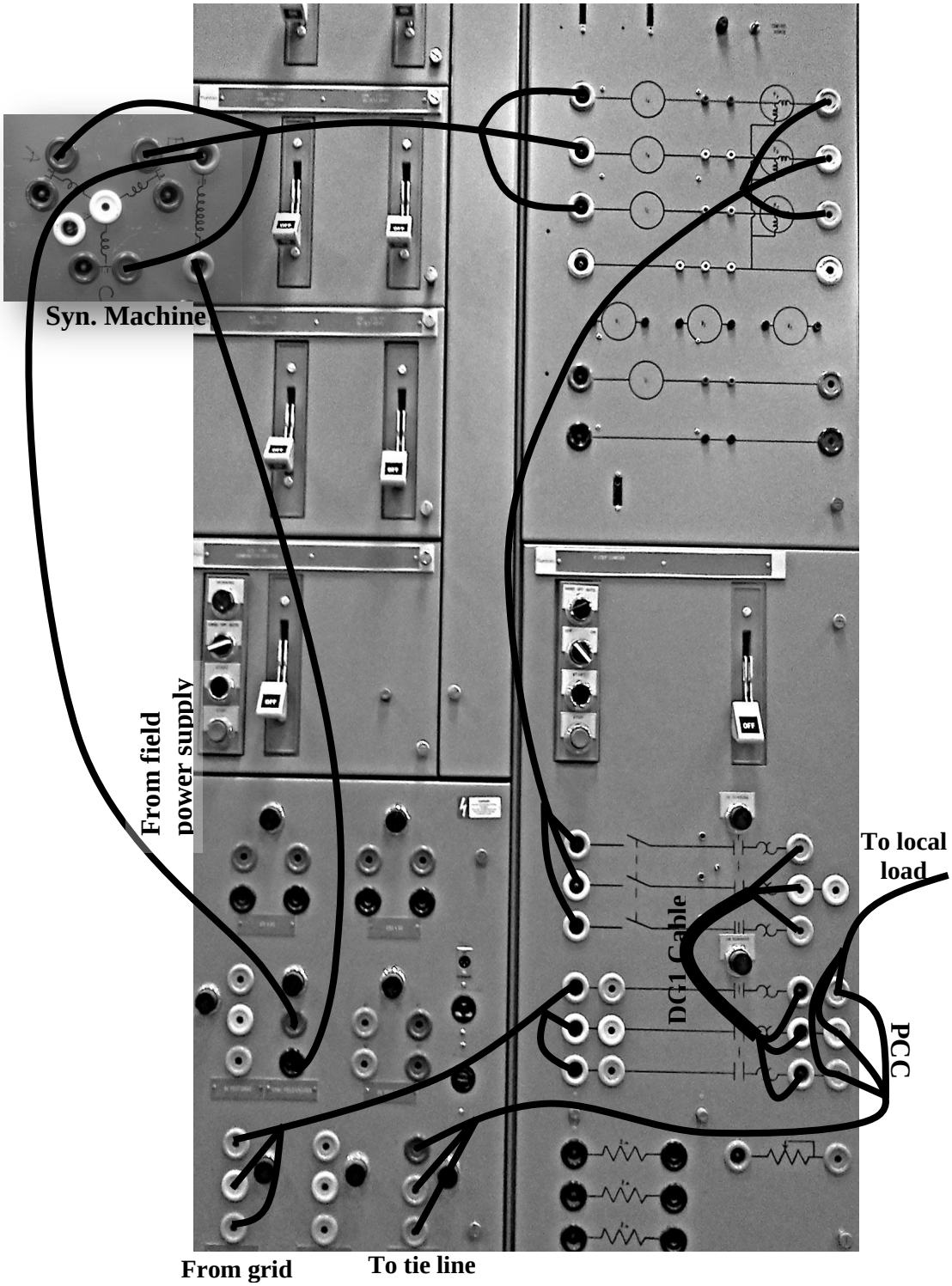

Figure B.2 DG1 wiring diagram

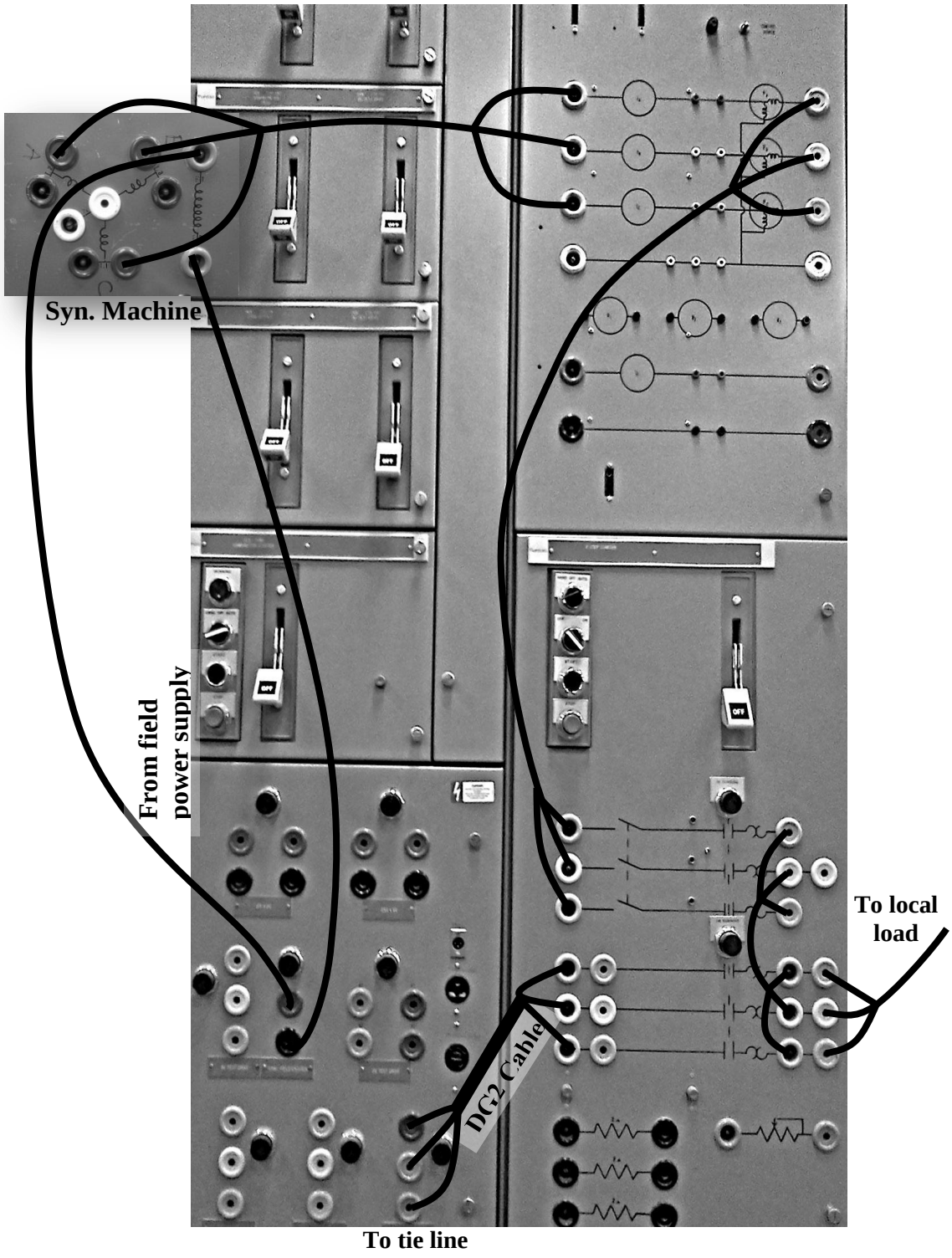

Figure B.3 DG2 wiring diagram

BIBLIOGRAPHY

[1] D. Moskovitz, "Profits and progress through distributed resources," *Regulatory Assistance Project, Tech. Rep.,* Feb. 2010.

[2] P. Dondi, D. Boyoumi, C. Haederli, D. Julian, M. Suter, "Network Integration of Distributed Power Generation," *J. Power Systems*, vol. 106, pp. 1–9, 2002.

[3] P. Piagi, R.H. Lasseter, "Autonomous Control of Microgrids," *IEEE PES Meeting,* 2006.

[4] IEEE Standards Coordination Committee 21, "IEEE Guide for Design, Operation, and Integration of Distributed Resource Island Systems with Electric Power Systems," 2011.

[5] J. A. P. Lopes, C. L. Moreira, and A. G. Madureira, "Defining Control Strategies for MicroGrids Islanded Operation," *IEEE Transactions on Power Systems*, vol. 21, no. 2, pp. 916–924, May 2006.

[6] In-Su Bae and Jin-O Kim, "Reliability Evaluation of Customers in a Microgrid," *IEEE Transactions on Power Systems*, vol. 23, no. 3, pp. 1416–1422, Aug. 2008.

[7] R. Martinez-Cid and E. O'Neill-Carrillo, "Sustainable microgrids for isolated systems," *IEEE PES Transmission and Distribution Conference and Exposition,* pp. 1 –7. 2010.

[8] C. Marnay, F. J. Robio, and A. S. Siddiqui, "Shape of the microgrid," IEEE *Power Engineering Society Winter Meeting*, vol. 1, pp. 150 –153, 2001.

[9] A. Llaria, O. Curea, J. Jimenez, H. Camblong, "Survey on microgrids: Unplanned islanding and related inverter control," *Intl. J. Renewable Energy*, vol. 36, pp. 2052–2061, 2011.

[10] N. D. Hatziargyriou, A. G. Anastasiadis, J. Vasiljevska, and A. G. Tsikalakis, "Quantification of economic, environmental and operational benefits of Microgrids," in *IEEE Bucharest PowerTech,* pp. 1 –8, 2009.

[11] P. Barker, D. Herman, "Technical And Economic Feasibility of Microgrid-Based Power Systems," *Seventh EPRI Distributed Resources Conference and Exhibition,* Mar. 2002.

[12] "Microgrids key to the smart grids evolution," *Power Engineering International*, vol. 18, no. 4, 2010.

[13]G. Venkataramanan and C. Marnay, "A larger role for microgrids," *IEEE Power and Energy Magazine,* vol. 6, no. 3, pp. 78–82, May 2008.

[14] D. Pudjianto and G. Strbac, "Large Scale Integration of Microgeneration to Low Voltage Grids, Work Package G: Regulatory regimes for supporting development of micro-grids," Prepared for the European Commission under contract # ENK5-CT-2002-00610.

[15] D. E. King, "Electric Power Microgrids: Opportunities and Challenges for an Emerging Distributed Energy Architecture," Carnegie Melon University, Pittsburg, 2006.

[16] M. A. Pedrasa and T. Spooner, "A survey of techniques used to control microgrid generation and storage during island operation," in *Australian Universities Power Engineering Conf*, 2006.

[17] M. Bollen, J. Zhong, and Y. Lin, "Performance indices and objectives for microgrids," in *20th International Conference and Exhibition on Electricity Distribution-Part 1*, pp. 1–4, 2009.

[18] F. A. Viawan and D. Karlsson, "Voltage and Reactive Power Control in Systems With Synchronous Machine-Based Distributed Generation," *IEEE Transactions on Power Delivery*, vol. 23, no. 2, pp. 1079–1087, Apr. 2008.

[19] C. Cho, J. Jeon, J. Kim, S. Kwon, K. Park, and S. Kim, "Active Synchronizing Control of a Microgrid," *IEEE Transactions on Power Electronics*, no. 99, pp. 1–1, 2011.

[20] D. G. Shendell, R. Prill, W. J. Fisk, M. G. Apte, D. Blake, and D. Faulkner, "Associations between classroom CO2 concentrations and student attendance in Washington and Idaho," *Indoor Air*, vol. 14, no. 5, pp. 333–341, 2004.

[21] R. H. Lasseter, "MicroGrids," in *Power Engineering Society Winter Meeting*, vol. 1, pp. 305–308, 2008.

[22] W. Yao, M. Chen, J. Matas, J. M. Guerrero, and Z.-M. Qian, "Design and Analysis of the Droop Control Method for Parallel Inverters Considering the Impact of the Complex Impedance on the Power Sharing," *IEEE Transactions on Industrial Electronics*, vol. 58, no. 2, pp. 576–588, Feb. 2011.

[23] T. L. Vandoorn, B. Meersman, J. D. M. De Kooning, and L. Vandevelde, "Directly-Coupled Synchronous Generators With Converter Behavior in Islanded Microgrids," *IEEE Transactions on Power Systems*, 2012.

[24] E. T. Andrade, P. E. M. J. Ribeiro, J. O. P. Pinto, C.-L. Chen, J.-S. Lai, and N. Kees, "A novel power calculation method for droop-control microgrid systems," in *Twenty-Seventh Annual IEEE Applied Power Electronics Conference and Exposition (APEC)*, pp. 2254 –2258, 2012.

[25] F. Pilo, G. Pisano, and G. G. Soma, “Neural implementation of microgrid central controllers,” in *Industrial Informatics, 2007 5th IEEE International Conference on*, 2007, vol. 2, pp. 1177–1182.

[26] A. L. Dimeas and N. D. Hatziargyriou, “Operation of a Multiagent System for Microgrid Control,” *IEEE Transactions on Power Systems*, vol. 20, no. 3, pp. 1447–1455, Aug. 2005.

[27] A. G. Tsikalakis and N. D. Hatziargyriou, “Centralized control for optimizing microgrids operation,” *IEEE Power and Energy Society General Meeting*, pp. 1 –8, 2007.

[28] A. A. Zaidi and F. Kupzog, “Microgrid automation-a self-configuring approach,” in *IEEE International Multitopic Conference*, pp. 565–570, 2007.

[29] S.-J. Ahn, J.-W. Park, I.-Y. Chung, S.-I. Moon, S.-H. Kang, and S.-R. Nam, “Power-Sharing Method of Multiple Distributed Generators Considering Control Modes and Configurations of a Microgrid,” *IEEE Transactions on Power Delivery*, vol. 25, no. 3, pp. 2007–2016, Jul. 2010.

[30] J. Jimeno, J. Anduaga, J. Oyarzabal, and A. G. de Muro, “Architecture of a microgrid energy management system,” *European Transactions on Electrical Power*, vol. 21, no. 2, pp. 1142–1158, 2011.

[31] H. J. Laaksonen, “Protection Principles for Future Microgrids,” *IEEE Transactions on Power Electronics*, vol. 25, no. 12, pp. 2910–2918, Dec. 2010.

VITA

Shyam Naren Bhaskara obtained his Bachelor of Technology degree in Electrical and Electronics Engineering from Jawaharlal Nehru Technological University, Hyderabad, India in May 2010. He received his Master of Science degree in Electrical Engineering from Missouri University of Science and Technology in Aug 2012. His research interests include power system operation and control, microgrids, and smart grids.